JOURNAL OF GUIDANCE, CONTROL, AND DYNAMICS
Vol. 27, No. 5, September–October 2004

Time Simulations of the Response of Maneuvering Flexible Aircraft

Leonard Meirovitch* and Ilhan Tuzcu†
Virginia Polytechnic Institute and State University, Blacksburg, Virginia 24061

This work is concerned with time simulations of the response of flying flexible aircraft to initial conditions and external excitations, such as gusts. The simulations are based on a unified formulation of the problem of dynamics and control of maneuvering flexible aircraft developed recently by the authors. The formulation represents a seamless integration of pertinent material from the areas of analytical dynamics, structural dynamics, aerodynamics, and controls. It incorporates both the aircraft rigid-body motions and elastic deformations and it includes the aerodynamic, propulsion, gravity, and control forces, all in a rigorous manner. The formulation lends itself to efficient computer processing of the aircraft response. The formulation contains improvements over the earlier formulation by the authors in the form of a reduced-order structural model and newly designed, easier-to-implement controller and state observer. The corresponding time simulations are entirely new, and no similar results have been obtained by other investigators. The developments should help with the design of the new generation of unmanned aerial vehicles (UAVs) and in particular with the design of autonomous UAVs controlled by autopilots.

Introduction

THIS paper is concerned with computer simulations of the response of flying flexible aircraft to initial conditions and external excitations. The problem formulation can be traced to generic equations of motion in terms of quasi-coordinates derived originally for flexible spacecraft[1] and extended subsequently to flexible aircraft.[2] Traditionally, the subject of stability and control of aircraft has been treated in two separate disciplines, flight dynamics[3] and aeroelasticity.[4] For the most part, flight dynamics is concerned with maneuvering rigid aircraft. Although on occasions some flexibility is included, flexible aircraft do not appear to be in the domain of flight dynamics. At the other end of the spectrum, aeroelasticity is concerned mostly with the vibration and flutter of flexible cantilevered wings. A few rigid-body degrees of freedom have sometimes been added in an ad hoc manner, but the subject of maneuvering flexible aircraft seems to have attracted little or no interest.

Over the past half century, there have been a number of attempts to treat flight dynamics and aeroelasticity on an integrated basis. Most of these attempts have been limited in scope, however, as the ultimate objective has been confined mainly to stability statements. The problem of simulating the dynamics and control of maneuvering flexible aircraft has been addressed in a comprehehsive manner quite recently.[5] Indeed, in Ref. 5 the authors integrate into a single consistent formulation all the material necessary for describing the dynamic response of maneuvering flexible aircraft, namely, analytical dynamics, structural dynamics, aerodynamics, and controls. Based on fundamental principles, the new unified theory incorporates in a rigorous manner both the rigid-body motions and the elastic deformations of the aircraft, as well as the aerodynamic, propulsion, gravity, and control forces, in addition to forces of an external nature. The formulation has been used in Ref. 5 to generate computer simulations of the response of flexible aircraft to a prescribed gust. Reference 5 contains a comprehensive review of the literature on the subject of combined flight dynamics and aeroelasticity of flexible aircraft. It should be pointed out, however, that virtually none of these investigations went so far as to simulate the flight of maneuvering flexible aircraft, so they are only marginally related.

It appears that two of the main stumbling blocks in developing a formulation capable of simulating the response of flying flexible aircraft are the difficulty in integrating various disciplines into a single unified formulation and the time required to carry out the necessary computations. These drawbacks are caused for the most part by the aerodynamics, which is difficult to integrate and demands a great deal of computer time. One aerodynamic theory not suffering from these drawbacks is strip theory; it is the theory used in Ref. 5 and in this paper. Time simulations of aircraft response to external stimuli of the type carried out in Ref. 5 can provide important information to the design process in general and to the design of autopilots in particular. Note that autopilots capable of controlling both rigid-body motions and elastic deformations ensure stable flight trajectories and passenger comfort, and by definition they prevent potential divergence and flutter. Moreover, they are essential to autonomous unmanned aerial vehicles (UAVs).

Computer simulations imply discrete-time computations, which raises the question of sampling period, or time step. For design purposes, the time required to compute the aerodynamic and control forces on line, to permit the computation of the system state at the next sampling time, need not bear much resemblance to the sampling period, although it should be reasonably short. For autopilots requiring real-time computations, the computational period must be the same as or shorter than the sampling period. Quite often, the difficulties in producing meaningful time simulations are due to the approach used. As an illustration, we cite Ref. 6, whose objective is to simulate "... fluid–structure interaction during rapid flight maneuvers at transonic conditions by use of advanced, time-accurate CFD–CSM coupling methodology." Essentially, "temporal and spatial coupling algorithms" are used in Ref. 6 to make two independent computer codes, one for aerodynamics (CFD) and the other for structural mechanics (CSM), work together. The scope of Ref. 6 is relatively limited, as the aircraft is assumed to follow a known preset trajectory, so that there are no rigid-body degrees of freedom and there are no controls. Not surprisingly, the process of meshing together two independently developed computer codes with large numbers of variables demands substantial time. Indeed, several relatively short-time simulations on a 32-processor computer took about 35 h.

This paper is concerned with time simulations of the response of flying flexible aircraft to external excitations and contains several

Presented as Paper 2003-1403 at the AIAA/ASME/ASCE/AHS/ASC 44th SDM Conference, Norfolk, VA, 7 April 2003; received 12 May 2003; revision received 9 January 2004; accepted for publication 12 January 2004.

*University Distinguished Professor Emeritus, Department of Engineering Science and Mechanics, MC 0219; lmeirovi@vt.edu. Fellow AIAA.

†Postdoctoral Research Associate, Department of Engineering Science and Mechanics, MC 0219; ituzcu@vt.edu. Member AIAA.

improvements over the formulation of Ref. 5. In particular, it involves a reduced-order structural model using whole-aircraft shape functions, instead of component shape functions as in Ref. 5, resulting in a 28-state model versus a 76-state model. Moreover, this paper involves new controller and observer designs. Superior performance of the controller and observer is achieved due to the lower-order model, as well as due to the addition of actuators and sensors placed at judiciously selected points throughout the aircraft. This is manifested through faster decay of the perturbed variables, faster convergence of the state observer, and significantly lower computational time. It should be pointed out that all the time simulations in this paper were carried out by a 1-GHz personal computer; every simulation took only a few minutes, which demonstrates the feasibility of real-time control. This is very important for autonomous UAVs, which must be controlled by autopilots and hence must have computers on board.

Equations of Motion in Terms of Component Generalized Coordinates

Aircraft can be regarded as assemblages of flexible components working together as single systems, where the components can be broadly identified as the fuselage (f), wing (w), and empennage (e). The motion of aircraft can be conveniently described by attaching sets of body axes $x_i y_i z_i (i = f, w, e)$ to the undeformed components (Fig. 1). Thus, the motion of the individual components can be described by three translations and three rotations of the body axes and elastic deformations measured relative to the body axes. Because the individual components do not move relative to one another, the translations and rotations of the wing body axes $x_w y_w z_w$ and empennage body axes $x_e y_e z_e$ are uniquely defined as soon as the translations and rotations of the fuselage body axes $x_f y_f z_f$, as well as the elastic deformations of the fuselage, are defined. Hence, we describe the motion of the aircraft as the translations and rotations of the fuselage body axes $x_f y_f z_f$ and the elastic displacements of nominal points of the individual components relative to the corresponding body axes.

From Ref. 5, the motion of a whole flexible aircraft of the type shown in Fig. 1 can be described by the position vector $\boldsymbol{R}_f(t)$ of the origin O_f of axes $x_f y_f z_f$ relative to the inertial axes XYZ, where $\boldsymbol{R}_f$ is expressed in terms of components along XYZ, a symbolic vector $\boldsymbol{\theta}_f(t)$ of Eulerian angles between $x_f y_f z_f$ and XYZ, and elastic displacement vectors $\boldsymbol{u}_i(\boldsymbol{r}_i, t)$ $(i = f, w, e)$ of typical points in the flexible components, in which $\boldsymbol{r}_i(x_i, y_i, z_i)$ are nominal position vectors relative to the origins O_i of the corresponding component body axes.

Because the elastic displacement vectors $\boldsymbol{u}_i(\boldsymbol{r}_i, t)$ depend on the spatial variables $\boldsymbol{r}_i$, the motion of the aircraft is described by ordinary differential equations for the translations and rotations of the reference frame $x_f y_f z_f$ and boundary-value problems[7] for the distributed variables $\boldsymbol{u}_i$. Note that boundary-value problems consist of partial differential equations and associated boundary conditions. Systems described by boundary-value problems are infinite-dimensional and for the most part they defy analytical solution. This is particularly true for the flexible aircraft under consideration, for which there is a boundary-value problem for each flexible component, and they are all coupled to each other, as well as to the ordinary differential equations for the rigid body motions. Hence, the only alternative is approximate solutions, which require spatial discretization[7] of the boundary-value problems. Rather than first deriving boundary-value problems and then carrying out spatial discretization, it is more efficient to discretize the distributed variables $\boldsymbol{u}_i$ directly. In either case, discretization amounts to approximating the distributed-parameter problems by finite sets of ordinary differential equations. To this end, we introduce the expansions

$$\boldsymbol{u}_i(\boldsymbol{r}_i, t) = \Phi_{ui}(\boldsymbol{r}_i)\boldsymbol{q}_{ui}(t), \qquad \psi_i(\boldsymbol{r}_i, t) = \Phi_{\psi i}(\boldsymbol{r}_i)\boldsymbol{q}_{\psi i}(t) \qquad i = f, w, e \tag{1}$$

where Φ_{ui} and $\Phi_{\psi i}$ are matrices of component shape functions and $\boldsymbol{q}_{ui}$ and $\boldsymbol{q}_{\psi i}$ are corresponding vectors of component generalized coordinates for bending and torsion, respectively. Then, adding some kinematical expressions relating time derivatives of displacements to quasi-velocities, Ref. 5 gives the special form of the state equations in terms of quasi-coordinates:

$$\begin{aligned}
&\dot{\boldsymbol{R}}_f = C_f^T \boldsymbol{V}_f, \qquad \dot{\boldsymbol{\theta}}_f = E_f^{-1}\boldsymbol{\omega}_f \\
&\dot{\boldsymbol{q}}_{ui} = \boldsymbol{s}_{ui}, \qquad \dot{\boldsymbol{q}}_{\psi i} = \boldsymbol{s}_{\psi i}, \qquad i = f, w, e \\
&\dot{\boldsymbol{p}}_{Vf} = -\tilde{\omega}_f \boldsymbol{p}_{Vf} + \boldsymbol{F}, \dot{\boldsymbol{p}}_{\omega f} = -\tilde{V}_f \boldsymbol{p}_{Vf} - \tilde{\omega}_f \boldsymbol{p}_{\omega f} + \boldsymbol{M} \\
&\left.\begin{aligned}
\dot{\boldsymbol{p}}_{ui} &= \frac{\partial T}{\partial \boldsymbol{q}_{ui}} - K_{ui}\boldsymbol{q}_{ui} - C_{ui}\boldsymbol{s}_{ui} + \boldsymbol{Q}_{ui} \\
\dot{\boldsymbol{p}}_{\psi i} &= -K_{\psi i}\boldsymbol{q}_{\psi i} - C_{\psi i}\boldsymbol{s}_{\psi i} + \boldsymbol{Q}_{\psi i}
\end{aligned}\right\} i = f, w, e
\end{aligned} \tag{2}$$

where $\boldsymbol{V}_f$, $\boldsymbol{\omega}_f$ are vectors of translational and angular quasi-velocities of $x_f y_f z_f$, $\tilde{V}_f$, $\tilde{\omega}_f$ are skew-symmetric matrices derived from $\boldsymbol{V}_f$, $\boldsymbol{\omega}_f$ (Ref. 8), C_f is a matrix of direction cosines between $x_f y_f z_f$ and XYZ, $\boldsymbol{s}_{ui}$, $\boldsymbol{s}_{\psi i}$ $(i = f, w, e)$ are component generalized velocities, $\boldsymbol{F}, \boldsymbol{M}$ are force and moment resultants due to gravity, aerodynamics, propulsion, controls, and external excitations acting on the whole aircraft and in terms of fuselage body axes components, T

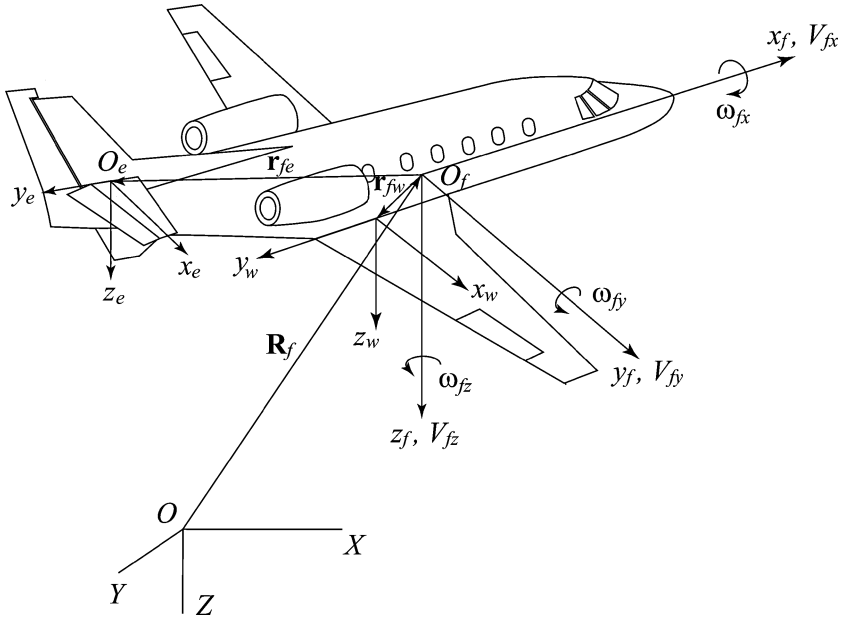

Fig. 1 Flying flexible aircraft.

is the kinetic energy for the whole aircraft, K_{ui}, $K_{\psi i}$ are component stiffness matrices for bending and torsion, C_{ui}, $C_{\psi i}$ are associated damping matrices, and $\boldsymbol{Q}_{ui}$, $\boldsymbol{Q}_{\psi i}$ are component generalized forces. Moreover,

$$\boldsymbol{p}_{Vf} = \frac{\partial T}{\partial \boldsymbol{V}_f}, \qquad \boldsymbol{p}_{\omega f} = \frac{\partial T}{\partial \boldsymbol{\omega}_f}$$

$$\boldsymbol{p}_{ui} = \frac{\partial T}{\partial \boldsymbol{s}_{ui}}, \qquad \boldsymbol{p}_{\psi i} = \frac{\partial T}{\partial \boldsymbol{s}_{\psi i}}, \qquad i = f, w, e \tag{3}$$

are associated momenta. Note that the term "quasi-coordinates" refers to the fact that the velocity vectors $\boldsymbol{V}_f$ and $\boldsymbol{\omega}_f$ cannot be integrated to obtain displacements and angular displacements,[8] where the components of $\boldsymbol{V}_f$ are referred to as forward velocity, sideslip, and plunge and the components of $\boldsymbol{\omega}_f$ are commonly known as roll, pitch, and yaw. It should be mentioned in passing that it was shown in Ref. 1 that the components of $\boldsymbol{V}_f$ can also be treated as quasi-coordinates. We observe that Eqs. (2) contain both velocities and momenta, so that the equations must be solved in conjunction with the associated momenta–velocities relations, which can be written in the compact form

$$\boldsymbol{p} = \frac{\partial T}{\partial \boldsymbol{V}} = M\boldsymbol{V} \tag{4}$$

where $\boldsymbol{p} = [\boldsymbol{p}_{Vf}^T \ \boldsymbol{p}_{\omega f}^T \ \boldsymbol{p}_{uf}^T \ \boldsymbol{p}_{uw}^T \ \cdots \ \boldsymbol{p}_{\psi e}^T]^T = [\boldsymbol{p}_1^T \ \boldsymbol{p}_2^T \ \boldsymbol{p}_3^T \ \boldsymbol{p}_4^T \ \cdots \ \boldsymbol{p}_8^T]^T$ is the system momentum vector, $\boldsymbol{V} = [\boldsymbol{V}_f^T \ \boldsymbol{\omega}_f^T \ \boldsymbol{s}_{uf}^T \ \boldsymbol{s}_{uw}^T \ \cdots \ \boldsymbol{s}_{\psi e}^T]^T = [\boldsymbol{V}_1^T \ \boldsymbol{V}_2^T \ \boldsymbol{V}_3^T \ \boldsymbol{V}_4^T \ \cdots \ \boldsymbol{V}_8^T]^T$ is the system velocity vector, and $M = [M_{ij}]$ is the system mass matrix, a symmetric matrix conveniently expressed in partitioned form with the submatrices[5]

$$M_{11} = mI, \qquad M_{12} = \tilde{S}^T$$

$$M_{13} = \int \Phi_{uf}\,\mathrm{d}m_f + \int C_w^T\left(\tilde{r}_w^T C_w \Delta\Phi_{ufw} + C_w\Phi_{ufw}\right)\mathrm{d}m_w + \int C_e^T\left(\tilde{r}_e^T C_e \Delta\Phi_{ufe} + C_e\Phi_{ufe}\right)\mathrm{d}m_e, \ldots,$$

$$M_{18} = C_e^T \int \tilde{r}_e^T \Phi_{\psi e}\,\mathrm{d}m_e, \qquad M_{22} = J$$

$$M_{23} = \int (\tilde{r}_f + \Phi_{uf}\widetilde{\boldsymbol{q}}_{uf})\Phi_{uf}\,\mathrm{d}m_f + \int \left[C_w(\tilde{r}_{fw} + \Phi_{ufw}\widetilde{\boldsymbol{q}}_{uf})^T + (\tilde{r}_w + \Phi_{uw}\widetilde{\boldsymbol{q}}_{uw})^T C_w\right]^T \left(\tilde{r}_w^T C_w \Delta\Phi_{ufw} + C_w\Phi_{ufw}\right)\mathrm{d}m_w + \int \left[C_e(\tilde{r}_{fe} + \Phi_{ufe}\widetilde{\boldsymbol{q}}_{uf})^T + (\tilde{r}_e + \Phi_{ue}\widetilde{\boldsymbol{q}}_{ue})^T C_e\right]^T \times \left(\tilde{r}_e^T C_e \Delta\Phi_{ufe} + C_e\Phi_{ufe}\right)\mathrm{d}m_e, \ldots,$$

$$M_{28} = \int \left[C_e(\tilde{r}_{fe} + \Phi_{ufe}\widetilde{\boldsymbol{q}}_{uf})^T + (\tilde{r}_e + \Phi_{ue}\widetilde{\boldsymbol{q}}_{ue})^T C_e\right]^T \tilde{r}_e^T \Phi_{\psi e}\,\mathrm{d}m_e$$

$$M_{33} = \int \Phi_{uf}^T\Phi_{uf}\,\mathrm{d}m_f + \int \left(\tilde{r}_w^T C_w \Delta\Phi_{ufw} + C_w\Phi_{ufw}\right)^T \times \left(\tilde{r}_w^T C_w \Delta\Phi_{ufw} + C_w\Phi_{ufw}\right)\mathrm{d}m_w + \int \left(\tilde{r}_e^T C_e \Delta\Phi_{ufe} + C_e\Phi_{ufe}\right)^T \left(\tilde{r}_e^T C_e \Delta\Phi_{ufe} + C_e\Phi_{ufe}\right)\mathrm{d}m_e$$

$$M_{34} = \int \left(\tilde{r}_w^T C_w \Delta\Phi_{ufw} + C_w\Phi_{ufw}\right)^T \Phi_{uw}\,\mathrm{d}m_w, \ldots,$$

$$M_{38} = \int \left(\tilde{r}_e^T C_e \Delta\Phi_{ufe} + C_e\Phi_{ufe}\right)^T \tilde{r}_e^T \Phi_{\psi e}\,\mathrm{d}m_e, \ldots,$$

$$M_{88} = \int \Phi_{\psi e}^T \tilde{r}_e \tilde{r}_e^T \Phi_{\psi e}\,\mathrm{d}m_e \tag{5}$$

in which m is the aircraft total mass,

$$\tilde{S} = \int (\tilde{r}_f + \Phi_{uf}\widetilde{\boldsymbol{q}}_{uf})\,\mathrm{d}m_f + \int \left[(\tilde{r}_{fw} + \Phi_{ufw}\widetilde{\boldsymbol{q}}_{uf})C_w^T + C_w^T(\tilde{r}_w + \Phi_{uw}\widetilde{\boldsymbol{q}}_{uw})\right]C_w\,\mathrm{d}m_w + \int \left[(\tilde{r}_{fe} + \Phi_{ufe}\widetilde{\boldsymbol{q}}_{uf})C_e^T + C_e^T(\tilde{r}_e + \Phi_{ue}\widetilde{\boldsymbol{q}}_{ue})\right]C_e\,\mathrm{d}m_e \tag{6}$$

is the matrix of first moments of inertia of the deformed aircraft, and

$$J = \int (\tilde{r}_f + \Phi_{uf}\widetilde{\boldsymbol{q}}_{uf})^T(\tilde{r}_f + \Phi_{uf}\widetilde{\boldsymbol{q}}_{uf})\,\mathrm{d}m_f + \int \left[C_w(\tilde{r}_{fw} + \Phi_{ufw}\widetilde{\boldsymbol{q}}_{uf})^T + (\tilde{r}_w + \Phi_{uw}\widetilde{\boldsymbol{q}}_{uw})^T C_w\right]^T \times \left[C_w(\tilde{r}_{fw} + \Phi_{ufw}\widetilde{\boldsymbol{q}}_{uf})^T + (\tilde{r}_w + \Phi_{uw}\widetilde{\boldsymbol{q}}_{uw})^T C_w\right]\mathrm{d}m_w + \int \left[C_e(\tilde{r}_{fe} + \Phi_{ufe}\widetilde{\boldsymbol{q}}_{uf})^T + (\tilde{r}_e + \Phi_{ue}\widetilde{\boldsymbol{q}}_{ue})^T C_e\right]^T \times \left[C_e(\tilde{r}_{fe} + \Phi_{ufe}\widetilde{\boldsymbol{q}}_{uf})^T + (\tilde{r}_e + \Phi_{ue}\widetilde{\boldsymbol{q}}_{ue})^T C_e\right]\mathrm{d}m_e \tag{7}$$

is the inertia matrix of the deformed aircraft. In the above

$$\Delta = \begin{bmatrix} 0 & 0 \\ 0 & -\dfrac{\partial}{\partial x_f} \\ \dfrac{\partial}{\partial x_f} & 0 \end{bmatrix}, \qquad \Phi_{uf} = \begin{bmatrix} \boldsymbol{0}^T & \boldsymbol{0}^T \\ \phi_{ufy}^T & \boldsymbol{0}^T \\ \boldsymbol{0}^T & \phi_{ufz}^T \end{bmatrix}$$

$$\Phi_{ufw} = \Phi_{uf}(\boldsymbol{r}_{fw}) \tag{8}$$

and expressions analogous to Φ_{uf} and Φ_{ufw} can be written for $\Phi_{\psi f}$ and $\Phi_{\psi fw}$. Consistent with the notation of Eq. (4), the kinetic energy has the simple form

$$T = \tfrac{1}{2}\boldsymbol{V}^T M\boldsymbol{V} \tag{9}$$

In Ref. 5 expressions are also given for $\partial T/\partial \boldsymbol{q}_{ui}$, the damping matrices C_{ui}, $C_{\psi i}$, and the stiffness matrices K_{ui}, $K_{\psi i}(i = f, w, e)$. Moreover, expressions for the generalized forces in terms of the actual distributed forces $\boldsymbol{f}_i(i = f, w, e)$ and the engine thrust $\boldsymbol{F}_E$ are given as follows:

$$\boldsymbol{F} = \int [\boldsymbol{f}_f + \boldsymbol{F}_E\delta(\boldsymbol{r}_f - \boldsymbol{r}_E)]\,\mathrm{d}D_f + C_w^T\int \boldsymbol{f}_w\,\mathrm{d}D_w + C_e^T\int \boldsymbol{f}_e\,\mathrm{d}D_e$$

$$\boldsymbol{M} = \int (\tilde{r}_f + \Phi_{uf}\widetilde{\boldsymbol{q}}_{uf})[\boldsymbol{f}_f + \boldsymbol{F}_E\delta(\boldsymbol{r}_f - \boldsymbol{r}_E)]\,\mathrm{d}D_f + \int [(\tilde{r}_{fw} + \Phi_{ufw}\widetilde{\boldsymbol{q}}_{uf})C_w^T + C_w^T(\tilde{r}_w + \Phi_{uw}\widetilde{\boldsymbol{q}}_{uw})]\boldsymbol{f}_w\,\mathrm{d}D_w + \int [(\tilde{r}_{fe} + \Phi_{ufe}\widetilde{\boldsymbol{q}}_{uf})C_e^T + C_e^T(\tilde{r}_e + \Phi_{ue}\widetilde{\boldsymbol{q}}_{ue})]\boldsymbol{f}_e\,\mathrm{d}D_e$$

$$\boldsymbol{Q}_{uf} = \int \Phi_{uf}^T[\boldsymbol{f}_f + \boldsymbol{F}_E\delta(\boldsymbol{r}_f - \boldsymbol{r}_E)]\,\mathrm{d}D_f + \int \left(\tilde{r}_w^T C_w \Delta\Phi_{ufw} + C_w\Phi_{ufw}\right)^T\boldsymbol{f}_w\,\mathrm{d}D_w + \int \left(\tilde{r}_e^T C_e \Delta\Phi_{ufe} + C_e\Phi_{ufe}\right)^T\boldsymbol{f}_e\,\mathrm{d}D_e$$

$$\boldsymbol{Q}_{\psi f} = \int \Phi_{\psi f}^T\tilde{r}_f[\boldsymbol{f}_f + \boldsymbol{F}_E\delta(\boldsymbol{r}_f - \boldsymbol{r}_E)]\,\mathrm{d}D_f + \int \left(\tilde{r}_w^T C_w\Phi_{\psi fw} + C_w\tilde{r}_{fw}^T\Phi_{\psi fw}\right)^T\boldsymbol{f}_w\,\mathrm{d}D_w + \int \left(\tilde{r}_e^T C_e\Phi_{\psi fe} + C_e\tilde{r}_{fe}^T\Phi_{\psi fe}\right)^T\boldsymbol{f}_e\,\mathrm{d}D_e$$

$$\boldsymbol{Q}_{ui} = \int \Phi_{ui}^T\boldsymbol{f}_i\,\mathrm{d}D_i, \qquad \boldsymbol{Q}_{\psi i} = \int \Phi_{\psi i}^T\tilde{r}_i\boldsymbol{f}_i\,\mathrm{d}D_i, \quad i = w, e \tag{10}$$

Equations of Motion in Terms of Aircraft Generalized Coordinates

In the dynamics and control of complex structures, such as the flexible aircraft under consideration (Fig. 1), structural modeling and structural control are subject to conflicting requirements. Accurate structural modeling tends to require a large number of degrees of freedom. There are two widely used discretization procedures capable of producing accurate structural models, the finite element method and the Galerkin method, the latter being equivalent to the Rayleigh–Ritz method for conservative systems.[7] The finite element method can accommodate very complex geometries but tends to require large numbers of degrees of freedom, reaching into many thousands. In contrast, the Galerkin method tends to require significantly fewer degrees of freedom, but its use is limited to relatively simple geometries. For example, using the Galerkin method, the flexible aircraft of Ref. 5 was modeled with 32 elastic degrees of freedom, which amounts to 38 degrees of freedom when the rigid-body motions are included. In this regard, it should be pointed out that, to demonstrate how the integration process works, it is not necessary to use models with complicated geometries. On the other side of the ledger, structural control design tends to experience increasing difficulties as the number of degrees of freedom of the model increases. Indeed, serious control design difficulties were experienced in Ref. 5 even though the model involved only 38 degrees of freedom, or 76 states, as discussed later in this paper.

From the preceding discussion, it follows that a smaller order structural model retaining a large measure of accuracy is highly desirable. In this paper, we consider the use of whole-aircraft shape functions, in contrast to the components shape functions used in Ref. 5. These aircraft shape functions can be obtained by solving an eigenvalue problem for the associated "free–free" aircraft structure undergoing small displacements from a given unstrained equilibrium state in the absence of aerodynamic forces. The eigenvalue problem just described can be written in the form

$$K\boldsymbol{d} = \lambda M_0 \boldsymbol{d} \tag{11}$$

where $K = \text{block-diag}[0 \;\; K_{uf} \;\; K_{uw} \;\; \cdots \;\; K_{\psi e}]$ is the symmetric positive semidefinite stiffness matrix for the whole system, in which 0 is a 6×6 null matrix corresponding to the rigid-body motions, $M_0 = M|_{q_{ui}=0}$ is a symmetric positive definite mass matrix consisting of the submatrices given by Eqs. (5) with the elastic displacement vectors $\boldsymbol{q}_{ui}$ $(i = f, w, e)$ set equal to zero, and $\boldsymbol{d} = [\boldsymbol{R}_f^T \;\; \boldsymbol{\theta}_f^T \;\; \boldsymbol{q}_{uf}^T \;\; \boldsymbol{q}_{uw}^T \;\; \cdots \;\; \boldsymbol{q}_{\psi e}^T]^T$ is the displacement vector for the associated linearized system, in which this time $\boldsymbol{\theta}_f$ is a genuine vector.

Assuming that there are n elastic degrees of freedom, the solution of the eigenvalue problem, Eq. (11), consists of $6+n$ eigenvalues λ_i and eigenvectors $\boldsymbol{d}_i$ $(i = 1, 2, \ldots, 6+n)$. Our objective is to reduce the dimension of the discretized system, which can be done only by reducing the number of elastic degrees of freedom. To this end, we retain only the first $6+m$ eigensolutions, the first 6 representing rigid-body eigenvectors with zero eigenvalues and the remaining m representing elastic eigenvectors with real positive eigenvalues, where m is significantly smaller than n. Then we replace the component generalized coordinate vectors $\boldsymbol{q}_{uf}(t)$, $\boldsymbol{q}_{uw}(t)$, $\ldots$, $\boldsymbol{q}_{\psi e}(t)$ with the aircraft generalized coordinates $\xi_1(t)$, $\xi_2(t)$, $\ldots$, $\xi_m(t)$, while leaving the rigid body coordinates unaffected. To carry out the necessary transformation, we introduce the notation $\boldsymbol{q}(t) = [\boldsymbol{q}_f^T \;\; \boldsymbol{q}_{uw}^T \;\; \cdots \;\; \boldsymbol{q}_{\psi e}^T]^T$, $\boldsymbol{s}(t) = [\boldsymbol{s}_{uf}^T \;\; \boldsymbol{s}_{uw}^T \;\; \cdots \;\; \boldsymbol{s}_{\psi e}^T]^T = [\dot{\boldsymbol{q}}_{uf}^T \;\; \dot{\boldsymbol{q}}_{uw}^T \;\; \cdots \;\; \dot{\boldsymbol{q}}_{\psi e}^T]^T$, $\boldsymbol{\xi}(t) = [\xi_1 \;\; \xi_2 \;\; \cdots \;\; \xi_m]^T$, $\boldsymbol{\eta}(t) = [\eta_1 \;\; \eta_2 \;\; \cdots \;\; \eta_m]^T = [\dot{\xi}_1 \;\; \dot{\xi}_2 \;\; \cdots \;\; \dot{\xi}_m]^T$ and write the truncated matrix of eigenvectors in the partitioned form

$$D = [\boldsymbol{d}_1 \;\; \boldsymbol{d}_2 \;\; \cdots \;\; \boldsymbol{d}_m] = \left[\begin{array}{c:c} I & X \\ \hdashline 0 & D_m \end{array}\right] \tag{12}$$

in which I is a 6×6 unit matrix, X is a $6\times m$ matrix of no particular interest, 0 is an $n\times 6$ null matrix, and D_m is an $n\times m$ matrix. Hence, consistent with the idea that the rigid-body variables are not to be affected, we write the desired transformation matrix as follows:

$$\boldsymbol{d}(t) = U\boldsymbol{d}_\xi(t), \qquad \boldsymbol{V}(t) = U\boldsymbol{V}_\eta(t) \tag{13}$$

where $\boldsymbol{d}(t) = [\boldsymbol{d}_r^T(t) \;\; \boldsymbol{q}^T(t)]^T$ and $\boldsymbol{d}_\xi(t) = [\boldsymbol{d}_r^T(t) \;\; \boldsymbol{\xi}^T(t)]^T$, in which $\boldsymbol{d}_r(t) = [\boldsymbol{R}_f^T(t) \;\; \boldsymbol{\theta}_f^T(t)]^T$ is the rigid-body displacement vector, and $\boldsymbol{V}(t) = [\boldsymbol{V}_r^T(t) \;\; \boldsymbol{s}^T(t)]^T$ and $\boldsymbol{V}_\eta(t) = [\boldsymbol{V}_r^T(t) \;\; \boldsymbol{\eta}^T(t)]^T$, in which $\boldsymbol{V}_r(t) = [\boldsymbol{V}_f^T(t) \;\; \boldsymbol{\omega}_f^T(t)]^T$ is the rigid-body velocity vector. Moreover,

$$U = \text{block-diag}\,[I \quad D_m] \tag{14}$$

is the transformation matrix. We refer to $\boldsymbol{d}_\xi(t)$ and $\boldsymbol{V}_\eta(t)$ as the reduced displacement vector and reduced velocity vector, respectively.

Next, we propose to derive the reduced-order state equations. To this end, we first write the mass matrix in the partitioned form

$$M = \left[\begin{array}{c:c} M_{rr} & M_{re} \\ \hdashline M_{re}^T & M_{ee} \end{array}\right] = M_q \tag{15}$$

insert the second of Eqs. (13) in conjunction with Eq. (14) into Eq. (9), express the kinetic energy as follows:

$$T = \tfrac{1}{2}\boldsymbol{V}^T M_q \boldsymbol{V} = \tfrac{1}{2}\boldsymbol{V}_\eta^T U^T M_q U \boldsymbol{V}_\eta = \tfrac{1}{2}\boldsymbol{V}_\eta^T M_\xi \boldsymbol{V}_\eta \tag{16}$$

in which

$$M_\xi = U^T M_q U = \left[\begin{array}{c:c} M_{rr} & M_{re}D_m \\ \hdashline D_m^T M_{re}^T & D_m^T M_{ee} D_m \end{array}\right] \tag{17}$$

is the reduced mass matrix associated with the aircraft generalized velocities, and note that M_ξ depends on $\boldsymbol{\xi}$. To derive the reduced stiffness matrix, we first introduce the notation $K_q = \text{block-diag}\,[K_{uf} \;\; K_{uw} \;\; \cdots \;\; K_{\psi e}]$ and write the potential energy

$$V = \tfrac{1}{2}\boldsymbol{q}^T K_q \boldsymbol{q} = \tfrac{1}{2}\boldsymbol{\xi}^T D_m^T K_q D_m \boldsymbol{\xi} = \tfrac{1}{2}\boldsymbol{\xi}^T K_\xi \boldsymbol{\xi} \tag{18}$$

so that the reduced stiffness matrix has the form

$$K_\xi = D_m^T K_q D_m \tag{19}$$

By analogy, the reduced damping matrix is given by

$$C_\eta = D_m^T C_s D_m \tag{20}$$

where $C_s = \text{block-diag}\,[C_{uf} \;\; C_{uw} \;\; \cdots \;\; C_{\psi e}]$.

Using the extended Hamilton principle[7] and adding the appropriate kinematical relations, we obtain the state equations for the reduced system in the form

$$\dot{\boldsymbol{R}}_f = C_f^T \boldsymbol{V}_f, \qquad \dot{\boldsymbol{\theta}}_f = E_f^{-1}\boldsymbol{\omega}_f, \qquad \dot{\boldsymbol{\xi}} = \boldsymbol{\eta}$$

$$\dot{\boldsymbol{p}}_{Vf} = -\tilde{\omega}_f \boldsymbol{p}_{Vf} + \boldsymbol{F}, \qquad \dot{\boldsymbol{p}}_{\omega f} = -\tilde{V}_f \boldsymbol{p}_{Vf} - \tilde{\omega}_f \boldsymbol{p}_{\omega f} + \boldsymbol{M}$$

$$\dot{\boldsymbol{p}}_\eta = \frac{\partial T}{\partial \boldsymbol{\xi}} - K_\xi \boldsymbol{\xi} - C_\eta \boldsymbol{\eta} + \boldsymbol{Q}_\xi \tag{21}$$

where, inserting the first of Eqs. (13) into Eqs. (10) and noting that $D_m = [D_{uf}^T \;\; D_{uw}^T \;\; \cdots \;\; D_{\psi e}^T]^T$, we obtain the generalized forces

$$\boldsymbol{F} = \int [\boldsymbol{f}_f + \boldsymbol{F}_E \delta(\boldsymbol{r}_f - \boldsymbol{r}_E)]\,\mathrm{d}D_f + C_w^T \int \boldsymbol{f}_w\,\mathrm{d}D_w + C_e^T \int \boldsymbol{f}_e\,\mathrm{d}D_e$$

$$\boldsymbol{M} = \int [\tilde{r}_f + (\Phi_{uf}\widetilde{D_{uf}\boldsymbol{\xi}})][\boldsymbol{f}_f + \boldsymbol{F}_E\delta(\boldsymbol{r}_f - \boldsymbol{r}_E)]\,\mathrm{d}D_f + \int \Big\{[(\tilde{r}_{fw} + (\Phi_{ufw}\widetilde{D_{uf}\boldsymbol{\xi}})]C_w^T + C_w^T[\tilde{r}_w + (\Phi_{uw}\widetilde{D_{uw}\boldsymbol{\xi}})]\Big\}\boldsymbol{f}_w\,\mathrm{d}D_w$$

$$+ \int \Big\{[\tilde{r}_{fe} + (\Phi_{ufe}\widetilde{D_{uf}\boldsymbol{\xi}})]C_e^T + C_e^T[(\tilde{r}_e + (\Phi_{ue}\widetilde{D_{ue}\boldsymbol{\xi}})]\Big\}\boldsymbol{f}_e\,\mathrm{d}De$$

$$\boldsymbol{Q}_\xi = \int \left(\Phi_{uf} D_{uf} + \tilde{r}_f^T \Phi_{\psi f} D_{\psi f}\right)^T [\boldsymbol{f}_f + \boldsymbol{F}_E \delta(\boldsymbol{r}_f - \boldsymbol{r}_E)]\, \mathrm{d}D_f$$

$$+ \int \left[\left(\tilde{r}_w^T C_w \Delta\Phi_{ufw} + C_w \Phi_{ufw}\right) D_{uf} + \Phi_{uw} D_{uw}\right.$$

$$\left. + \left(\tilde{r}_w^T C_w + C_w \tilde{r}_{fw}^T\right)\Phi_{\psi fw} D_{\psi f} + \tilde{r}_w^T \Phi_{\psi w} D_{\psi w}\right]^T \boldsymbol{f}_w\, \mathrm{d}D_w$$

$$+ \int \left[\left(\tilde{r}_e^T C_e \Delta\Phi_{ufe} + C_e \Phi_{ufe}\right) D_{uf} + \Phi_{ue} D_{ue}\right.$$

$$\left. + \left(\tilde{r}_e^T C_e + C_e \tilde{r}_{fe}^T\right)\Phi_{\psi fe} D_{\psi f} + \tilde{r}_e^T \Phi_{\psi e} D_{\psi e}\right]^T \boldsymbol{f}_e\, \mathrm{d}D_e \tag{22}$$

in which a tilde over a vector expression inside parentheses denotes a skew-symmetric matrix formed from the vector expression in question,[8] and the same applies to all similar expressions appearing in this paper. Moreover, using a process similar to that used in Ref. 5, it can be shown that

$$\frac{\partial T}{\partial \boldsymbol{\xi}} = D_{uf}^T \left[\int \Phi_{uf}^T \tilde{\omega}_f^T \bar{\boldsymbol{V}}_f\, \mathrm{d}m_f + \Phi_{ufw}^T \tilde{\omega}_f^T C_w^T \int \bar{\boldsymbol{V}}_w\, \mathrm{d}m_w\right.$$

$$\left. + \Phi_{ufe}^T \tilde{\omega}_f^T C_e^T \int \bar{\boldsymbol{V}}_e\, \mathrm{d}m_e\right] + D_{uw}^T \int \Phi_{uw}^T (\widetilde{C_w \boldsymbol{\omega}_f})^T \bar{\boldsymbol{V}}_w\, \mathrm{d}m_w$$

$$+ D_{ue}^T \int \Phi_{ue}^T (\widetilde{C_e \boldsymbol{\omega}_f})^T \bar{\boldsymbol{V}}_e\, \mathrm{d}m_e \tag{23}$$

in which

$$\bar{\boldsymbol{V}}_f(\boldsymbol{r}_f, t) = \boldsymbol{V}_f + [\tilde{r}_f + (\Phi_{uf} \widetilde{D_{uf}} \boldsymbol{\xi})]^T \boldsymbol{\omega}_f$$

$$+ \left(\Phi_{uf} D_{uf} + \tilde{r}_f^T \Phi_{\psi f} D_{\psi f}\right)\boldsymbol{\eta}$$

$$\bar{\boldsymbol{V}}_w(\boldsymbol{r}_w, t) = C_w \boldsymbol{V}_f + \left\{C_w [\tilde{r}_{fw} + (\Phi_{ufw} \widetilde{D_{uf}} \boldsymbol{\xi})]^T\right.$$

$$\left. + [\tilde{r}_w + (\Phi_{uw} \widetilde{D_{uw}} \boldsymbol{\xi})]^T C_w\right\}\boldsymbol{\omega}_f$$

$$+ \left[\left(\tilde{r}_w^T C_w \Delta\Phi_{ufw} + C_w \Phi_{ufw}\right) D_{uf} + \Phi_{uw} D_{uw}\right.$$

$$\left. + \left(\tilde{r}_w^T C_w + C_w^T \tilde{r}_{fw}^T\right)\Phi_{\psi fw} D_{\psi f} + \tilde{r}_w^T \Phi_{\psi w} D_{\psi w}\right]\boldsymbol{\eta} \tag{24}$$

are velocity vectors of typical points in the aircraft components, and we note that an expression for $\bar{\boldsymbol{V}}_e(\boldsymbol{r}_e, t)$ can be obtained from $\bar{\boldsymbol{V}}_w(\boldsymbol{r}_w, t)$ by simply replacing the subscript w by e. Because Eqs. (21) contain both velocities and momenta, they must be solved in conjunction with the momenta–velocities relation

$$\boldsymbol{p} = M_\xi V_\eta \tag{25}$$

where $\boldsymbol{p} = [\boldsymbol{p}_{Vf}^T \;\; \boldsymbol{p}_{\omega f}^T \;\; \boldsymbol{p}_\eta^T]^T$ is the system momentum vector.

It is perhaps appropriate to pause at this point and examine the relation between component shape functions and aircraft shape functions. Of course, both classes of functions represent admissible functions[7] and can be used in conjunction with Galerkin's method for the spatial discretization of the partial differential equations describing the elastic deformations of the aircraft. Quite often, component shape functions are chosen in the form of the eigenfunctions of an elastic member closely related to the component in question, for which reason they are frequently referred to as component modes. If the structure lends itself to a Galerkin discretization, then the model derived by means of component shape functions tends to require significantly fewer degrees of freedom than a finite element model for comparable accuracy. Still, the number of degrees of freedom using component shape functions is not nearly as small as that of a model derived by means of aircraft shape functions. In essence, aircraft shape functions represent linear combinations of component shape functions, as can be concluded from the first of Eqs. (13). These linear combinations, obtained by solving the eigenvalue problem given by Eq. (11), are such that the resulting aircraft shape functions can represent accurately the mass and stiffness properties of the aircraft structure with fewer degrees of freedom than the arbitrary combinations of component shape functions chosen originally. In spite of the fact that they were obtained by solving an eigenvalue problem, the aircraft shape functions are not really aircraft modes. Indeed, the idea of aircraft modes implies not merely structural discretization but decoupling of the equations of motion, and hence the ability to solve the decoupled equations independently. In fact, because the mass matrix depends on the elastic deformations, rather than being constant, and the aircraft is subjected to structural damping and aerodynamic forces, the aircraft shape functions, whether referred to as modes or not, do not decouple the equations of motion. The real reason for our use of aircraft shape functions is to generate a discrete model of the aircraft structure with a relatively small number of degrees of freedom, which is of vital importance to feedback control design.

In approximating a distributed-parameter system by a discrete model, a question arising frequently relates to the number of elastic degrees of freedom needed to ensure that the system is sufficiently accurate for the derivation of system response and control design. In this regard, basing the model on aircraft shape functions has many advantages. Whereas the aircraft shape functions do not represent aircraft modes, they do possess features similar to those of modes, such as frequencies and shapes. In view of this, and using the analogy with conservative systems, we include in the model the shape functions corresponding to the lowest frequencies first and keep on adding shape functions corresponding to increasing frequencies as the participation in the response warrants. This procedure is based on the fact that the participation decreases as the frequencies increase, where the rate of decrease depends on the nature of the structure.[7] Moreover, the shape of the functions, and in particular the location of the nodes, provides clues as to the placement of actuators and sensors to ensure controllability and observability.[9]

The preceding discussion of reduced-order structural modeling is predicated on spatial discretization by the Galerkin method. Yet the finite element method is by far the discretization technique of choice, so that the interest lies in producing a relatively low-dimensional aircraft model based on the finite element method. This would require the solution of the corresponding eigenvalue problem. But mass and stiffness matrices for models derived by the finite element method tend to be of very high dimension. Fortunately, a complete solution of the eigenvalue problem is not really necessary, as the interest lies in only a limited number of lower eigenvectors. These eigenvectors are then used in conjunction with the associated interpolation functions to generate the corresponding aircraft shape functions. From here on, the procedure for deriving the reduced-order state equations is the same as that for the Galerkin discretization described earlier.

Perturbation Approach to the Aircraft Response

The state equations, Eqs. (21), represent a set of nonlinear differential equations whose order depends on the number of elastic degrees of freedom of the model. A solution of these equations can encounter serious difficulties due to the system nonlinearities and the fact that the rigid-body variables tend to be large compared to the elastic variables. Moreover, if the number of elastic degrees of freedom is large, even if only moderately so, the control design is likely to experience problems. These difficulties can be obviated by adopting a perturbation approach[5] to the problem, based on the aircraft dynamics. In the case at hand, this amounts to assuming that the quantities associated with the aircraft rigid-body motions can be expressed as the sum of a large part, called the zero-order part, and a small part, called the first-order part, as follows:

$$\boldsymbol{R}_f = \boldsymbol{R}_f^{(0)} + \boldsymbol{R}_f^{(1)}, \qquad \boldsymbol{\theta}_f = \boldsymbol{\theta}_f^{(0)} + \boldsymbol{\theta}_f^{(1)}, \qquad \boldsymbol{V}_f = \boldsymbol{V}_f^{(0)} + \boldsymbol{V}_f^{(1)}$$

$$\boldsymbol{\omega}_f = \boldsymbol{\omega}_f^{(0)} + \boldsymbol{\omega}_f^{(1)}, \qquad \boldsymbol{p}_{Vf} = \boldsymbol{p}_{Vf}^{(0)} + \boldsymbol{p}_{Vf}^{(1)}, \qquad \boldsymbol{p}_{\omega f} = \boldsymbol{p}_{\omega f}^{(0)} + \boldsymbol{p}_{\omega f}^{(1)}$$

$$\boldsymbol{F} = \boldsymbol{F}^{(0)} + \boldsymbol{F}^{(1)}, \qquad \boldsymbol{M} = \boldsymbol{M}^{(0)} + \boldsymbol{M}^{(1)} \tag{26}$$

in which the zero-order quantities, denoted by the superscript (0), are at least one order of magnitude larger than the first-order quantities, denoted by (1). Moreover, the quantities associated with the elastic

deformations are assumed to be of first order. With this understanding, we omit the superscript from the elastic quantities. Inserting Eqs. (26) into Eqs. (21), considering the fact that the elastic quantities are of first order, and separating different orders of magnitude, we obtain the state equations for the zero-order problem

$$\dot{\boldsymbol{R}}_f^{(0)} = C_f^{(0)T}\boldsymbol{V}_f^{(0)}, \qquad \dot{\boldsymbol{\theta}}_f^{(0)} = \left(E_f^{(0)}\right)^{-1}\boldsymbol{\omega}_f^{(0)}$$

$$\dot{\boldsymbol{p}}_{Vf}^{(0)} = -\tilde{\omega}_f^{(0)}\boldsymbol{p}_{Vf}^{(0)} + \boldsymbol{F}^{(0)}, \qquad \dot{\boldsymbol{p}}_{\omega f}^{(0)} = -\tilde{V}_f^{(0)}\boldsymbol{p}_{Vf}^{(0)} - \tilde{\omega}_f^{(0)}\boldsymbol{p}_{\omega f}^{(0)} + \boldsymbol{M}^{(0)} \tag{27}$$

where the matrices $C_f^{(0)}$ and $E_f^{(0)}$ are as given in Ref. 5. Moreover, from the first two of Eqs. (22), the zero-order generalized forces have the expressions

$$\boldsymbol{F}^{(0)} = \int \left[\boldsymbol{f}_f^{(0)} + \boldsymbol{F}_E^{(0)}\delta(\boldsymbol{r}_f - \boldsymbol{r}_E)\right] \mathrm{d}D_f + C_w^T \int \boldsymbol{f}_w^{(0)}\,\mathrm{d}D_w + C_e^T \int \boldsymbol{f}_e^{(0)}\,\mathrm{d}D_e$$

$$\boldsymbol{M}^{(0)} = \int \tilde{r}_f\left[\boldsymbol{f}_f^{(0)} + \boldsymbol{F}_E^{(0)}\delta(\boldsymbol{r}_f - \boldsymbol{r}_E)\right] \mathrm{d}D_f + \int \left(\tilde{r}_{fw}C_w^T + C_w^T\tilde{r}_w\right)\boldsymbol{f}_w^{(0)}\,\mathrm{d}D_w + \int \left(\tilde{r}_{fe}C_e^T + C_e^T\tilde{r}_e\right)\boldsymbol{f}_e^{(0)}\,\mathrm{d}D_e \tag{28}$$

in which $\boldsymbol{f}_f^{(0)}, \boldsymbol{f}_w^{(0)}$, and $\boldsymbol{f}_e^{(0)}$ are actual distributed zero-order forces acting on the individual components; their expressions are also given in Ref. 5. Equations (27) contain both momenta and velocities, so that they must be solved in conjunction with the zero-order momenta–velocities relation. From Eqs. (17) and (25), in the absence of elastic deformations, this relation can be written as

$$\boldsymbol{p}^{(0)} = \boldsymbol{p}_r^{(0)} = M_{rr}^{(0)}\boldsymbol{V}_r^{(0)} \tag{29}$$

which reduces to

$$\boldsymbol{p}_{Vf}^{(0)} = m\boldsymbol{V}_f^{(0)} + \tilde{S}^{(0)T}\boldsymbol{\omega}_f^{(0)}, \qquad \boldsymbol{p}_{\omega f}^{(0)} = \tilde{S}^{(0)}\boldsymbol{V}_f^{(0)} + J^{(0)}\boldsymbol{\omega}_f^{(0)} \tag{30}$$

where the notation is obvious. We observe that Eqs. (27)–(29) describe the motion of the aircraft as if it were rigid; we refer to them as the flight dynamics problem.

The perturbation technique also yields the state equations for the first-order problem

$$\dot{\boldsymbol{R}}_f^{(1)} = C_f^{(0)T}\boldsymbol{V}_f^{(1)} + C_f^{(1)T}\boldsymbol{V}_f^{(0)}$$

$$\dot{\boldsymbol{\theta}}_f^{(1)} = \left(E_f^{(0)}\right)^{-1}\boldsymbol{\omega}_f^{(1)} - \left(E_f^{(0)}\right)^{-1}E_f^{(1)}\left(E_f^{(0)}\right)^{-1}\boldsymbol{\omega}_f^{(0)}, \qquad \dot{\boldsymbol{\xi}} = \boldsymbol{\eta}$$

$$\dot{\boldsymbol{p}}_{Vf}^{(1)} = -\tilde{\omega}_f^{(1)}\boldsymbol{p}_{Vf}^{(0)} - \tilde{\omega}_f^{(0)}\boldsymbol{p}_{Vf}^{(1)} + \boldsymbol{F}^{(1)}$$

$$\dot{\boldsymbol{p}}_{\omega f}^{(1)} = -\tilde{V}_f^{(1)}\boldsymbol{p}_{Vf}^{(0)} - \tilde{V}_f^{(0)}\boldsymbol{p}_{Vf}^{(1)} - \tilde{\omega}_f^{(1)}\boldsymbol{p}_{\omega f}^{(0)} - \tilde{\omega}_f^{(0)}\boldsymbol{p}_{\omega f}^{(1)} + \boldsymbol{M}^{(1)}$$

$$\dot{\boldsymbol{p}}_\eta = \left(\frac{\partial T}{\partial \boldsymbol{\xi}}\right)^{(1)} - K_\xi\boldsymbol{\xi} - C_\eta\boldsymbol{\eta} + \boldsymbol{Q}_\xi \tag{31}$$

in which the matrices $C_f^{(1)}$ and $E_f^{(1)}$ are as given in Ref. 5. Moreover, from Eqs. (22), the first-order generalized forces have the expressions

$$\boldsymbol{F}^{(1)} = \int \left[\boldsymbol{f}_f^{(1)} + \boldsymbol{F}_E^{(1)}\delta(\boldsymbol{r}_f - \boldsymbol{r}_E)\right] \mathrm{d}D_f + C_w^T \int \boldsymbol{f}_w^{(1)}\,\mathrm{d}D_w + C_e^T \int \boldsymbol{f}_e^{(1)}\,\mathrm{d}D_e$$

$$\boldsymbol{M}^{(1)} = \int \left\{\tilde{r}_f\left[\boldsymbol{f}_f^{(1)} + \boldsymbol{F}_E^{(1)}\delta(\boldsymbol{r}_f - \boldsymbol{r}_E)\right] + (\Phi_{uf}\widetilde{D_{uf}}\boldsymbol{\xi})\left[\boldsymbol{f}^{(0)} + \boldsymbol{F}_E^{(0)}\delta(\boldsymbol{r}_f - \boldsymbol{r}_E)\right]\right\} \mathrm{d}D_f + \int \left\{\left(\tilde{r}_{fw}C_w^T + C_w^T\tilde{r}_w\right)\boldsymbol{f}_w^{(1)} + \left[\left(\Phi_{ufw}\widetilde{D_{uf}}\boldsymbol{\xi}\right)C_w^T + C_w^T(\Phi_{uw}\widetilde{D_{uw}}\boldsymbol{\xi})\right]\boldsymbol{f}_w^{(0)}\right\} \mathrm{d}D_w + \int \left\{\left(\tilde{r}_{fe}C_e^T + C_e^T\tilde{r}_e\right)\boldsymbol{f}_e^{(1)} + \left[(\Phi_{ufe}\widetilde{D_{uf}}\boldsymbol{\xi})C_e^T + C_e^T(\Phi_{ue}\widetilde{D_{ue}}\boldsymbol{\xi})\right]\boldsymbol{f}_e^{(0)}\right\} \mathrm{d}D_e$$

$$\boldsymbol{Q}_\xi = \int \left(\Phi_{uf}D_{uf} + \tilde{r}_f^T\Phi_{\psi f}D_{\psi f}\right)^T\left[\boldsymbol{f}_f^{(0)} + \boldsymbol{f}_f^{(1)} + \left(\boldsymbol{F}_E^{(0)} + \boldsymbol{F}_E^{(1)}\right)\delta(\boldsymbol{r}_f - \boldsymbol{r}_E)\right] \mathrm{d}D_f + \int \left[\left(\tilde{r}_w^T C_w\Delta\Phi_{ufw} + C_w\Phi_{ufw}\right)D_{uf} + \Phi_{uw}D_{uw} + \left(\tilde{r}_w^T C_w + C_w\tilde{r}_{fw}^T\right)\Phi_{\psi fw}D_{\psi f} + \tilde{r}_w^T\Phi_{\psi w}D_{\psi w}\right]^T\left(\boldsymbol{f}_w^{(0)} + \boldsymbol{f}_w^{(1)}\right) \mathrm{d}D_w + \int \left[\left(\tilde{r}_e^T C_e\Delta\Phi_{ufe} + C_e\Phi_{ufe}\right)D_{uf} + \Phi_{ue}D_{ue} + \left(\tilde{r}_e^T C_e + C_e\tilde{r}_{fe}^T\right)\Phi_{\psi fe}D_{\psi f} + \tilde{r}_e^T\Phi_{\psi e}D_{\psi e}\right]^T\left(\boldsymbol{f}_e^{(0)} + \boldsymbol{f}_e^{(1)}\right) \mathrm{d}D_e \tag{32}$$

where $\boldsymbol{f}_f^{(1)}$, $\boldsymbol{f}_w^{(1)}$, and $\boldsymbol{f}_e^{(1)}$ are given in Ref. 5. In addition,

$$\left(\frac{\partial T}{\partial \boldsymbol{\xi}}\right)^{(1)} = D_{uf}^T\left\{\int \Phi_{uf}^T\left(\tilde{\omega}_f^{(0)T}\bar{\boldsymbol{V}}_f^{(1)} + \tilde{\omega}_f^{(1)T}\bar{\boldsymbol{V}}_f^{(0)}\right) \mathrm{d}m_f + \Phi_{ufw}^T\left[\tilde{\omega}_f^{(0)T}C_w^T\int \bar{\boldsymbol{V}}_w^{(1)}\,\mathrm{d}m_w + \tilde{\omega}_f^{(1)T}C_w^T\int \bar{\boldsymbol{V}}_w^{(0)}\,\mathrm{d}m_w\right] + \Phi_{ufe}^T\left[\tilde{\omega}_f^{(0)T}C_e^T\int \bar{\boldsymbol{V}}_e^{(1)}\,\mathrm{d}m_e + \tilde{\omega}_f^{(1)T}C_e^T\int \bar{\boldsymbol{V}}_e^{(0)}\,\mathrm{d}m_e\right]\right\} + D_{uw}^T\int \Phi_{uw}^T\left[\left(C_w\widetilde{\boldsymbol{\omega}}_f^{(0)}\right)^T\bar{\boldsymbol{V}}_w^{(1)} + \left(C_w\widetilde{\boldsymbol{\omega}}_f^{(1)}\right)^T\bar{\boldsymbol{V}}_w^{(0)}\right] \mathrm{d}m_w + D_{ue}^T\int \Phi_{ue}^T\left[\left(C_e\widetilde{\boldsymbol{\omega}}_f^{(0)}\right)^T\bar{\boldsymbol{V}}_e^{(1)} + \left(C_e\widetilde{\boldsymbol{\omega}}_f^{(1)}\right)^T\bar{\boldsymbol{V}}_e^{(0)}\right] \mathrm{d}m_e \tag{33}$$

in which

$$\bar{\boldsymbol{V}}_f^{(0)} = \boldsymbol{V}_f^{(0)} + \tilde{r}_f^T\boldsymbol{\omega}_f^{(0)}$$

$$\bar{\boldsymbol{V}}_f^{(1)} = \boldsymbol{V}_f^{(1)} + \tilde{r}_f^T\boldsymbol{\omega}_f^{(1)} + (\Phi_{uf}\widetilde{D_{uf}}\boldsymbol{\xi})^T\boldsymbol{\omega}_f^{(0)} + \left(\Phi_{uf}D_{uf} + \tilde{r}_f^T\Phi_{\psi f}D_{\psi f}\right)\boldsymbol{\eta}$$

$$\bar{\boldsymbol{V}}_w^{(0)} = C_w\boldsymbol{V}_f^{(0)} + \left(C_w\tilde{r}_{fw}^T + \tilde{r}_w^T C_w\right)\boldsymbol{\omega}_f^{(0)}$$

$$\bar{\boldsymbol{V}}_w^{(1)} = C_w\boldsymbol{V}_f^{(1)} + \left(C_w\tilde{r}_{fw}^T + \tilde{r}_w^T C_w\right)\boldsymbol{\omega}_f^{(1)} + \left[C_w(\Phi_{ufw}\widetilde{D_{uf}}\boldsymbol{\xi})^T + (\Phi_{uw}\widetilde{D_{uw}}\boldsymbol{\xi})^T C_w\right]\boldsymbol{\omega}_f^{(0)} + \left[\left(\tilde{r}_w^T C_w\Delta\Phi_{ufw} + C_w\Phi_{ufw}\right)D_{uf} + \Phi_{uw}D_{uw} + \left(\tilde{r}_w^T C_w + C_w\tilde{r}_{fw}^T\right)\Phi_{\psi fw}D_{\psi f} + \tilde{r}_w^T\Phi_{\psi w}D_{\psi w}\right]\boldsymbol{\eta} \tag{34}$$

and we note that expressions for $\bar{\boldsymbol{V}}_e^{(0)}$ and $\bar{\boldsymbol{V}}_e^{(1)}$ can be obtained by simply replacing w by e in $\bar{\boldsymbol{V}}_w^{(0)}$ and $\bar{\boldsymbol{V}}_w^{(1)}$, respectively.

Equations (31) contain both momenta and velocities, so that they must be augmented by an appropriate momenta–velocities relation. To this end, we retain the first-order terms in Eq. (25) and obtain the desired relation in the form

$$\boldsymbol{p}^{(1)} = M_\xi^{(0)}\boldsymbol{V}_\eta^{(1)} + M_\xi^{(1)}\boldsymbol{V}_\eta^{(0)} \tag{35}$$

in which $\boldsymbol{p}^{(1)} = [\boldsymbol{p}_{Vf}^{(1)T}\ \boldsymbol{p}_{\omega f}^{(1)T}\ \boldsymbol{p}_\eta^T]^T$ is the first-order momentum vector, $\boldsymbol{V}_\eta^{(0)} = [\boldsymbol{V}_f^{(0)T}\ \boldsymbol{\omega}_f^{(0)T}\ \boldsymbol{0}^T]^T$ is the $(6+m)$-dimensional zero-order

velocity vector, $\boldsymbol{V}_\eta^{(1)} = [\boldsymbol{V}_f^{(1)T} \;\; \boldsymbol{\omega}_f^{(1)T} \;\; \boldsymbol{\eta}^T]^T$ is the first-order velocity vector, and

$$M_\xi^{(0)} = \left[\begin{array}{cc:c} mI & \tilde{S}^{(0)T} & \\ \tilde{S}^{(0)} & J^{(0)} & M_{re}^{(0)} D_m \\ \hdashline & & \\ D_m^T M_{re}^{(0)T} & & D_m^T M_{ee}^{(0)} D_m \end{array}\right]$$

$$M_\xi^{(1)} = \left[\begin{array}{cc:c} 0 & \tilde{S}^{(1)T} & \\ \tilde{S}^{(1)} & J^{(1)} & M_{re}^{(1)} D_m \\ \hdashline & & \\ D_m^T M_{re}^{(1)T} & & D_m^T M_{ee}^{(1)} D_m \end{array}\right] \tag{36}$$

are the $(6+m) \times (6+m)$ zero-order and first-order mass matrices.

Equations (31)–(36) represent an extended perturbation problem. The equations include in a natural manner the perturbations in all six rigid-body motions of the aircraft. Moreover, the equations contain terms representing the solution of the zero-order problem, or flight dynamics problem, which implies physically that the extended perturbation problem is subject to excitations due to aircraft maneuvers. But, because there is a whole variety of possible aircraft maneuvers, the first-order equations represent an entire family of extended perturbation problems, one problem for every maneuver. We note that, to accommodate all possible maneuvers, the motions in the extended perturbation problem are measured relative to a noninertial set of body axes. Hence, in general the inputs from maneuvers inject time-varying terms into the extended perturbation problem. A notable exception is when the aircraft undergoes steady level flight, in which case the reference frame is inertial and the inputs do not depend on time.

Control Design

In general, aircraft must follow a given flight path. To realize this flight path, the pilot must control the trajectory and the attitude of the aircraft by setting the angles of the control surfaces and the engines throttles. This implies that Eqs. (27) actually represent an inverse dynamics problem, which requires the solution of nonlinear algebraic equations rather than the solution of nonlinear differential equations. Because of various disturbances, such as those due to wind, the aircraft often deviates from the desired flight path. If left unchecked, these deviations can lead to gross errors in the flight path, particularly the deviations in the rigid-body angular motions. Moreover, the elastic vibration can cause human discomfort. To ensure that all perturbations from the desired flight path are driven to zero, they are controlled closed loop, i.e., by means of feedback control. The corresponding control design is based on the extended perturbation equations, Eqs. (31).

The solution of state equations is most conveniently carried out in matrix form. Addressing the flight dynamics problem first, we solve the zero-order momenta–velocities relation, Eq. (29), or Eqs. (30), for the velocity vector $\boldsymbol{V}_r^{(0)} = [\boldsymbol{V}_f^{(0)T} \; \boldsymbol{\omega}_f^{(0)T}]^T$, introduce the result into Eqs. (27), and write the zero-order state equations in the compact form

$$\dot{\boldsymbol{x}}^{(0)}(t) = \boldsymbol{f}\big(\boldsymbol{x}^{(0)}(t)\big) + B^{(0)}\big(\boldsymbol{x}^{(0)}(t)\big)\boldsymbol{u}^{(0)}(t) \tag{37}$$

where $\boldsymbol{f}$ is a nonlinear vector function of the zero-order state $\boldsymbol{x}^{(0)} = [\boldsymbol{R}_f^{(0)T} \;\; \boldsymbol{\theta}_f^{(0)T} \;\; \boldsymbol{p}_{Vf}^{(0)T} \;\; \boldsymbol{p}_{\omega f}^{(0)T}]^T$, $B^{(0)}$ is a coefficient matrix with the top half equal to the null matrix, and $\boldsymbol{u}^{(0)} = [F_E^{(0)} \;\; \delta_a^{(0)} \;\; \delta_e^{(0)} \;\; \delta_r^{(0)}]^T$ is the control vector, in which $F_E^{(0)}$ is the engine thrust and $\delta_a^{(0)}$, $\delta_e^{(0)}$, and $\delta_r^{(0)}$ are the aileron, elevator, and rudder angles, respectively. As indicated, Eq. (37) represents an inverse dynamics problem in the sense that first a state vector $\boldsymbol{x}^{(0)}(t)$ describing a desired aircraft maneuver is postulated and then a control vector $\boldsymbol{u}^{(0)}(t)$ permitting realization of the given maneuver is determined.

In a similar fashion, solving the first-order momenta–velocities relation, Eq. (35), for the velocity vector $\boldsymbol{V}_\eta^{(1)} = [\boldsymbol{V}_f^{(1)T} \;\; \boldsymbol{\omega}_f^{(1)T} \;\; \boldsymbol{\eta}^T]^T$ and inserting the result into Eqs. (31), we can write the first-order state equations in the compact form

$$\dot{\boldsymbol{x}}^{(1)}(t) = A(t)\boldsymbol{x}^{(1)}(t) + B(t)\boldsymbol{u}^{(1)}(t) + [0 \quad I]^T \boldsymbol{F}_{\text{ext}}(t) \tag{38}$$

where $\boldsymbol{x}^{(1)} = [\boldsymbol{R}_f^{(1)T} \;\; \boldsymbol{\theta}_f^{(1)T} \;\; \boldsymbol{\xi}^T \;\; \boldsymbol{p}_{Vf}^{(1)T} \;\; \boldsymbol{p}_{\omega f}^{(1)T} \;\; \boldsymbol{p}_\eta^T]^T$ is the first-order state vector, $A(t)$ and $B(t)$ are coefficient matrices, $\boldsymbol{u}^{(1)} = [F_E^{(1)} \;\; \delta_a^{(1)} \;\; \delta_e^{(1)} \;\; \delta_r^{(1)} \;\; f_{w1}^R \;\; f_{w2}^R \;\; f_{w1}^L \;\; f_{w2}^L \;\; f_{e1}^R \;\; f_{e2}^R \;\; f_{e1}^L \;\; f_{e2}^L \;\; f_{e1}^V \;\; f_{e2}^V]^T$ is the first-order control vector, in which f_{w1}^R and f_{w2}^R are actuator forces located on the right half of the wing and paralled to z_w^R, f_{w1}^L and f_{w2}^L are similar actuator forces on the left half, f_{e1}^R, f_{e2}^R, f_{e1}^L and f_{e2}^L are actuator forces on the horizontal stabilizer, and f_{e1}^V and f_{e2}^V are actuator forces on the vertical stabilizer, and $\boldsymbol{F}_{\text{ext}}$ is a vector of generalized external forces.

The control design amounts to determining the control vector $\boldsymbol{u}^{(1)}$ such that, for any excitation $\boldsymbol{F}_{\text{ext}}$ of relatively short duration, the state vector $\boldsymbol{x}^{(1)}$ tends to zero with time. A technique yielding an optimal $\boldsymbol{u}^{(1)}$ is the linear quadratic regulator (LQR) method,[9] where $\boldsymbol{u}^{(1)}$ is obtained by minimizing the quadratic performance measure

$$J = \frac{1}{2}\int_0^{t_f} \Big[\boldsymbol{x}^{(1)T}(t) Q(t) \boldsymbol{x}^{(1)}(t) + \boldsymbol{u}^{(1)T}(t) \boldsymbol{R}(t) \boldsymbol{u}^{(1)}(t)\Big]\, \mathrm{d}t \tag{39}$$

in which $Q(t)$ is a real symmetric positive semidefinite matrix, $R(t)$ is a real symmetric positive definite matrix, and t_f is the final control time. The resulting control law is given by

$$\boldsymbol{u}^{(1)}(t) = -G(t)\boldsymbol{x}^{(1)}(t) \tag{40}$$

where

$$G(t) = R^{-1}(t) B^T(t) K(t) \tag{41}$$

is the control gain matrix, in which $K(t)$ is a real symmetric matrix satisfying the transient Riccati equation,[9] a matrix differential equation. Inserting Eq. (40) into Eq. (38), we obtain the closed-loop state equation

$$\dot{\boldsymbol{x}}^{(1)}(t) = [A(t) - B(t)G(t)]\boldsymbol{x}^{(1)}(t) + [0 \quad I]^T \boldsymbol{F}_{\text{ext}}(t) \tag{42}$$

In the special case in which the coefficient matrices A and B, as well as the weighting matrices R and Q in the performance measure,[9] are all constant and the final time t_f is relatively large, K tends to a constant matrix with time, in which case the Riccati equation reduces to the steady-state Riccati equation, an algebraic equation. Then, for $\boldsymbol{F}_{\text{ext}} = \boldsymbol{0}$, Eq. (42) reduces to

$$\dot{\boldsymbol{x}}^{(1)}(t) = (A - BG)\boldsymbol{x}^{(1)}(t) \tag{43}$$

which has the exponential solution $\boldsymbol{x}^{(1)}(t) = e^{\lambda t}\boldsymbol{x}^{(1)}$, where λ and $\boldsymbol{x}^{(1)}$ are constants satisfying the closed-loop eigenvalue problem

$$A_c \boldsymbol{x}^{(1)} = \lambda \boldsymbol{x}^{(1)} \tag{44}$$

in which $A_c = A - BG$ is the closed-loop coefficient matrix. The closed loop system is asymptotically stable if all the eigenvalues λ_i $(i = 1, 2, \ldots, 2(6+m))$ are real and negative and/or complex conjugates with negative real part.

The solution of the eigenvalue problem, Eq. (44), and in particular the eigenvalues, is sufficient to determine the stability of the closed-loop system, Eq. (43). To simulate the system response to initial and external excitations, it is necessary to integrate the state equations, Eq. (42). For a constant closed-loop matrix, $A_c = A - BG = \text{constant}$, the system response can be expressed in the form of the convolution integral[9]

$$\boldsymbol{x}^{(1)}(t) = e^{A_c t}\boldsymbol{x}^{(1)}(0) + \int_0^t e^{A_c(t-\tau)}[0 \quad I]^T \boldsymbol{F}_{\text{ext}}(\tau)\, \mathrm{d}\tau \tag{45}$$

where $\boldsymbol{x}^{(1)}(0)$ is the initial state vector and $e^{A_c t}$ is the transition matrix, a matrix that can be expressed in the form of the series

$$e^{A_c t} = I + tA_c + (t^2/2!)A_c^2 + (t^3/3!)A_c^3 + \cdots \tag{46}$$

In the case in which A_c depends on time, the solution of Eq. (42) can be obtained numerically in discrete time.[9]

Before the control gain matrix G can be computed, it is necessary to choose the weighting matrices Q and R appearing in the performance measure, Eq. (39). Although in theory the LQR method guarantees asymptotic stability of the closed-loop system, in practice there are choices of Q and R that fail to produce a solution. In such cases, it may be possible to obtain a reasonable solution by a trial-and-error process. This process is likely to be made significantly easier by the reduced-order modeling described earlier in this paper.

Control via Stochastic Estimator

Implementation of the control law, Eq. (40), requires the first-order state $\boldsymbol{x}^{(1)}$, which must be obtained from measurements. We observe, however, that the state vector contains generalized displacements and momenta, which are abstract quantities, and the measurements are all real quantities. Hence, the state can only be inferred from measurements, which can be done by means of an estimator, or observer.

We assume that the measurement vector can be written as

$$\boldsymbol{y}(t) = \boldsymbol{y}^{(0)}(t) + \boldsymbol{y}^{(1)}(t) \tag{47}$$

where the zero-order part $\boldsymbol{y}^{(0)}$ is obtained by means of an inertial navigation system consisting of three accelerometers and three gyros mounted on an inertial platform; the first-order part $\boldsymbol{y}^{(1)}$ is obtained by means of N_i sensors ($i = f, w, e$) measuring velocities at points P_k ($k = 1, 2, \ldots, N_i$) of the aircraft components. The interest lies in estimating the first-order state $\boldsymbol{x}^{(1)}(t)$ from the first-order measurement vector $\boldsymbol{y}^{(1)}(t)$, where the latter is referred to as the output vector; the relation between the two can be written as

$$\boldsymbol{y}^{(1)}(t) = C\boldsymbol{x}^{(1)}(t) \tag{48}$$

in which C is a matrix to be determined later in this section.

As indicated earlier, the state vector $\boldsymbol{x}^{(1)}(t)$ can only be estimated by means of an observer, which represents a dynamical system similar to the actual system and described by[9]

$$\dot{\hat{\boldsymbol{x}}}^{(1)}(t) = A\hat{\boldsymbol{x}}^{(1)}(t) + B\boldsymbol{u}^{(1)}(t) + K_o[\boldsymbol{y}^{(1)}(t) - C\hat{\boldsymbol{x}}^{(1)}(t)] \tag{49}$$

where $\hat{\boldsymbol{x}}^{(1)}(t)$ is the observer state and K_o is an observer gain matrix. Letting $\boldsymbol{F}_{\text{ext}} = \boldsymbol{0}$ in Eq. (38), subtracting Eq. (49) from the result, and introducing the observer error vector $\boldsymbol{e}(t) = \boldsymbol{x}^{(1)}(t) - \hat{\boldsymbol{x}}^{(1)}(t)$, we obtain the observer error equation

$$\dot{\boldsymbol{e}}(t) = (A - K_o C)\boldsymbol{e}(t) \tag{50}$$

The objective is to determine the observer gain matrix K_o such that the error goes to zero with time. This is ensured if all the eigenvalues of the matrix $A - K_o C$ are real and negative and/or are complex conjugates with negative real part.

In implementing the controls, we must feed back the observer state, because the actual state is not available. Hence, we must replace the control law given by Eq. (40) by the control law

$$\boldsymbol{u}^{(1)}(t) = -G\hat{\boldsymbol{x}}^{(1)}(t) \tag{51}$$

If the eigenvalues of the matrix $A - K_o C$ lie deep in the left half of the complex plane, then the observer state converges rapidly to the actual state, thus ensuring good accuracy of the response simulations.

An optimal observer can be obtained by means of a stochastic approach whereby the observer gain matrix K_o is determined by solving a matrix Riccati equation based on two correlation matrices, V and W, the first associated with the state excitation noise, including the actuator noise, and the second associated with the observation noise, or sensor noise. The stochastic observer is known as the Kalman–Bucy filter[9] and is the type of observer used in this paper.

There remains the question of determing the matrix C, which in the case at hand is not a trivial matter. Using the velocity sensors and their locations as indicated earlier, the output vector has the form $\boldsymbol{y}^{(1)}(t) = [\boldsymbol{R}_f^{(1)T}(t)\ \boldsymbol{\theta}_f^{(1)T}(t)\ \boldsymbol{y}_f^{(1)T}(t)\ \boldsymbol{y}_w^{(1)T}(t)\ \boldsymbol{y}_e^{(1)T}(t)]^T$, where $\boldsymbol{y}_i^{(1)}(t) = [\bar{\boldsymbol{V}}_i^{(1)T}(P_1, t)\ \bar{\boldsymbol{V}}_i^{(1)T}(P_2, t)\ \cdots\ \bar{\boldsymbol{V}}_i^{(1)T}(P_{N_i}, t)]^T$ ($i = f, w, e$), in which $\bar{\boldsymbol{V}}_i^{(1)}(P_k, t)$ are vectors of velocity measurements. From the second of Eqs. (34), we can write

$$\begin{aligned}\bar{\boldsymbol{V}}_f^{(1)}(P_k, t) &= \boldsymbol{V}_f^{(1)}(t) + \tilde{r}_f^T(P_k)\boldsymbol{\omega}_f^{(1)}(t) + \tilde{\omega}_f^{(0)}\Phi_{uf}(P_k)D_{uf}\boldsymbol{\xi}(t) \\ &\quad + \left[\Phi_{uf}(P_k)D_{uf} + \tilde{r}_f^T(P_k)\Phi_{\psi f}(P_k)D_{\psi f}\right]\boldsymbol{\eta}(t) \\ &= C_{fk}\begin{bmatrix}\boldsymbol{d}_\xi^{(1)}(t) \\ \boldsymbol{V}_\eta^{(1)}(t)\end{bmatrix}, \qquad k = 1, 2, \ldots, N_f\end{aligned} \tag{52}$$

where

$$\begin{aligned}C_{fk} = \big[&0 \quad 0 \quad \tilde{\omega}_f^{(0)}\Phi_{uf}(P_k)D_{uf} \quad I \quad \tilde{r}_f^T(P_k) \\ &\Phi_{uf}(P_k)D_{uf} + \tilde{r}_f^T(P_k)\Phi_{\psi f}(P_k)D_{\psi f}\big]\end{aligned} \tag{53}$$

Similarly, from the fourth of Eqs. (34), we can write

$$\bar{\boldsymbol{V}}_w^{(1)}(P_k, t) = \text{block-diag}\, C_{wk}\begin{bmatrix}\boldsymbol{d}_\xi^{(1)}(t) \\ \boldsymbol{V}_\eta^{(1)}(t)\end{bmatrix}, \quad k = 1, 2, \ldots, N_w \tag{54}$$

in which

$$\begin{aligned}C_{wk} = \big[&0 \quad 0 \quad C_w\tilde{\omega}_f^{(0)}\Phi_{ufw}D_{uf} + \big(\widetilde{C_w\boldsymbol{\omega}_f^{(0)}}\big)\Phi_{uw}(P_k)D_{uw} \\ &C_w \quad C_w\tilde{r}_{fw}^T + \tilde{r}_w^T(P_k)C_w \quad \big(\tilde{r}_w^T(P_k)C_w\Delta\Phi_{ufw} \\ &+ C_w\Phi_{ufw}\big)D_{uf} + \Phi_{uw}(P_k)D_{uw} + \big(\tilde{r}_w^T(P_k)C_w \\ &+ C_w\tilde{r}_{fw}^T\big)\Phi_{\psi fw}D_{\psi f} + \tilde{r}_w^T(P_k)\Phi_{\psi w}(P_k)D_{\psi w}\big]\end{aligned} \tag{55}$$

Moreover, $\bar{\boldsymbol{V}}_e^{(1)}(P_k, t)$ can be obtained from Eqs. (54) and (55) by simply replacing w by e.

Equations (52) and (54) are in terms of $\boldsymbol{d}_\xi^{(1)}$ and $\boldsymbol{V}_\eta^{(1)}$. They can be transformed into equations in terms of the state $\boldsymbol{x}^{(1)}$ by using Eq. (35) and writing

$$\begin{bmatrix}\boldsymbol{d}_\xi^{(1)}(t) \\ \boldsymbol{V}_\eta^{(1)}(t)\end{bmatrix} = \begin{bmatrix}I & 0 \\ -\left(M_\xi^{(0)}\right)^{-1}M_V & \left(M_\xi^{(0)}\right)^{-1}\end{bmatrix}\boldsymbol{x}^{(1)} \tag{56}$$

where, because $M_\xi^{(1)} = M_\xi^{(1)}(\boldsymbol{\xi})$, we used the relation $M_\xi^{(1)}\boldsymbol{V}_\eta^{(0)} = M_V\boldsymbol{d}_\xi^{(1)}$. Finally, using Eqs. (52), (54), and (56), we conclude that

$$C = \begin{bmatrix}I & 0 & 0 & \cdots & 0 \\ 0 & I & 0 & \cdots & 0 \\ & & C_{f1} & & \\ & & C_{f2} & & \\ & & \cdots\cdots\cdots & & \\ & & C_{fN_f} & & \\ & & C_{w1} & & \\ & & C_{w2} & & \\ & & \cdots\cdots\cdots & & \\ & & C_{wN_w} & & \\ & & C_{e1} & & \\ & & C_{e2} & & \\ & & \cdots\cdots\cdots & & \\ & & C_{eN_e} & &\end{bmatrix}\begin{bmatrix}I & 0 \\ -\left(M_\xi^{(0)}\right)^{-1}M_V & \left(M_\xi^{(0)}\right)^{-1}\end{bmatrix} \tag{57}$$

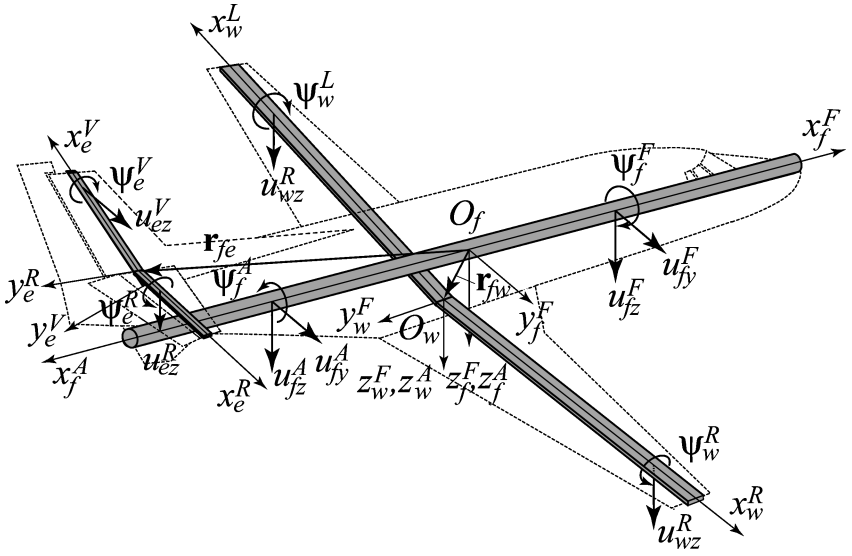

Fig. 2 Aircraft components undergoing bending and torsion.

Numerical Example

We consider the flexible aircraft shown in Fig. 1, and in particular the model depicted in Fig. 2. It is the same model as that considered in Ref. 5, from which we obtain the mass matrix M and stiffness matrix K corresponding to spatial discretization by means of aircraft component shape functions. Then, forming the matrix $M_0 = M|_{q=0}$ and solving the small-motions eigenvalue problem, Eq. (11), we obtain the eigenvectors $\boldsymbol{d}_1, \boldsymbol{d}_2, \ldots, \boldsymbol{d}_{6+n}$ and associated eigenvalues $\lambda_1, \lambda_2, \ldots, \lambda_{6+n}$, and we note that the first six are the rigid-body eigenvectors with zero eigenvalues. Removing the first six rows and columns from the matrix of eigenvectors and retaining only m columns, we obtain the $n \times m$ matrix D_m of elastic eigenvectors, as indicated by Eq. (12). These elastic eigenvectors represent aircraft shape functions; the first two are plotted in Fig. 3. Then, using Eqs. (13) and (14), we reduce the order of the state equations to $2(6+m)$; the reduced system is given by Eqs. (21).

The objective is to produce time simulations of the aircraft response. This task is rendered significantly simpler by the perturbation approach described earlier whereby the state equations are separated into a flight dynamics problem, Eqs. (27), and an extended perturbation problem, Eqs. (31). The first describes quasi-rigid aircraft maneuvers and the second the feedback control of deviations from these maneuvers. We consider two cases, steady level flight and a level steady turn maneuver.

A. Steady Level Flight

Steady level flight, described by the zero-order problem, is defined by

$$\boldsymbol{V}_f^{(0)} = C_f^{(0)}[V^{(0)} \quad 0 \quad 0] = \text{const.}, \qquad \boldsymbol{\omega}_f^{(0)} = \boldsymbol{0} \tag{58}$$

where $V^{(0)}$ is the aircraft forward velocity, so that Eqs. (30) reduce to

$$\boldsymbol{p}_{Vf}^{(0)} = m\boldsymbol{V}_f^{(0)} = \text{const.}, \qquad \boldsymbol{p}_{\omega f}^{(0)} = \tilde{S}^{(0)}\boldsymbol{V}_f^{(0)} = \text{const.} \tag{59}$$

Then, from the second line of Eqs. (27), we conclude that

$$\boldsymbol{F}^{(0)} = \boldsymbol{0}, \qquad \boldsymbol{M}^{(0)} = \boldsymbol{0} \tag{60}$$

which indicate that the aerodynamic, gravity, propulsion, and control forces balance out to zero.

We consider a flight at an altitude of 25,000 ft and with a forward velocity of 416.67 ft/s and hence a Mach number of 0.41. Assuming that the roll angle $\phi^{(0)}$, yaw angle $\psi^{(0)}$, aileron angle $\delta_a^{(0)}$, and rudder angle $\delta_r^{(0)}$ are all zero and solving the nonlinear equations (59), we obtain the pitch angle, which is equal to the angle of attack, $\theta^{(0)} = 3.82$ deg, the engine thrust $F_E^{(0)} = 431.6465$ lb, and the elevator angle $\delta_e^{(0)} = -15.49$ deg. Note that expressions for the aerodynamic, gravity, propulsion, and control forces entering into $\boldsymbol{F}^{(0)}$ and $\boldsymbol{M}^{(0)}$ are given in Ref. 5.

In the case of steady level flight, the aircraft experiences small static deformations due to the zero-order forces. The procedure for calculating them is given in Ref. 5, although here there is the added

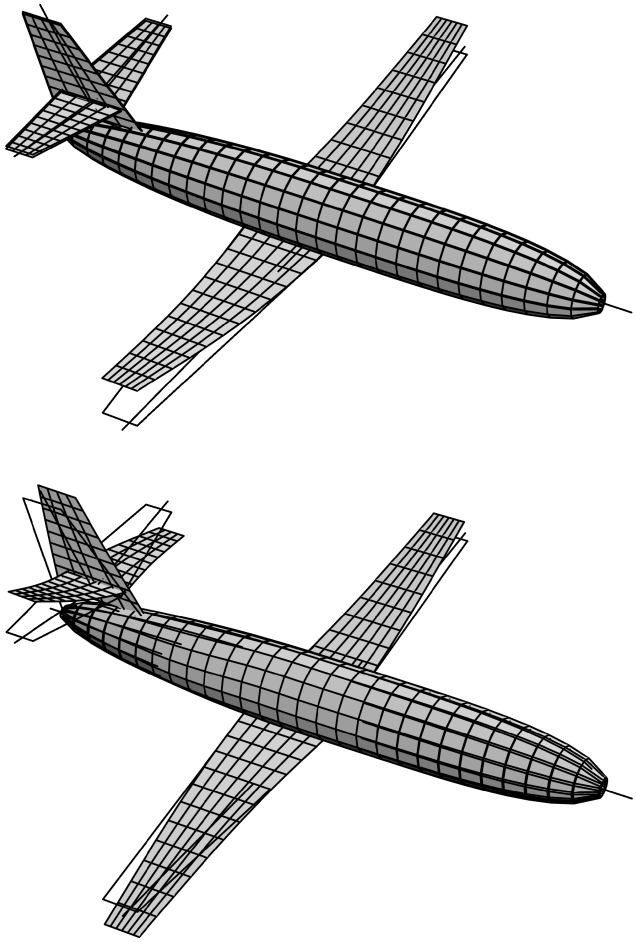

Fig. 3 First two aircraft shape functions.

task of transforming displacements in terms of component shape functions into displacements in terms of aircraft shape functions.

For the reduced model, we use $m = 8$ aircraft shape functions and compute the system matrices A and B in the extended perturbation problem defined by Eq. (38). Note that eight aircraft shape functions are quite sufficient to represent accurately the system dynamic characteristics. Implicit in this statement is the fact that the aircraft shape functions associated with the higher eigenvalues are increasingly "wrinkled" and hence increasingly difficult to excite. Moreover, because the lower shape functions have few nodes, it would be extremely difficult to place all the sensors and actuators at the nodes of the eight shape functions, so that observability and controllability are virtually assured on physical grounds. The control vector $\boldsymbol{u}^{(1)}$ is of dimension 14; the actuators are listed in the paragraph below Eq. (38). A trial-and-error process yielded the choice of the weighting matrices $Q = \text{diag}[1\ \ 1\ \ \cdots\ \ 1\ \ 0\ \ 0\ \ \cdots\ \ 0]$ and $R = \text{diag}[0.03\ \ 2 \times 10^6\ \ 10^6\ \ 10^6\ \ 1\ \ 1\ \ \cdots\ \ 1]$ appearing in the performance measure, Eq. (39). Then, solving the corresponding steady-state Riccati equation and using Eq. (41), we obtain the control gain matrix

$$G = \left[\begin{array}{ccccccc} 5.7305 & 0 & 0.6976 & 0.0032 & \cdots & 0 & 0 \\ 0 & 0.0005 & 0 & 0.3563 & \cdots & 0 & 0 \\ -0.0001 & 0 & 0.0007 & 0 & \cdots & 0 & 0 \\ 0 & 0.0001 & 0 & 0.0370 & \cdots & 0 & 0 \\ 0.0089 & 0.3552 & -0.0200 & 280.6827 & \cdots & -0.0002 & 0.0018 \\ 0.0034 & 0.3578 & 0.0296 & 281.7501 & \cdots & -0.0002 & 0.0018 \\ 0.0089 & -0.3552 & -0.0200 & -280.6829 & \cdots & 0.0002 & -0.0018 \\ \hline 0 & -0.0585 & 0 & -9.6674 & \cdots & 0 & -0.0001 \\ 0 & 0.0040 & 0 & 25.0041 & \cdots & 0 & 0.0001 \end{array}\right] \tag{61}$$

Note that the reduction in the system order rendered the process of choosing Q and R much easier. Then, solving the eigenvalue problem (44), we obtain the closed-loop eigenvalues

$$\lambda_{1,2} = -0.4094 \pm 0.4050i, \qquad \lambda_{3,4} = -0.3836 \pm 0.5937i$$
$$\lambda_5 = -0.7686, \qquad \lambda_{6,7} = -1.1873 \pm 0.7906i,$$
$$\ldots, \lambda_{27,28} = -9.3168 \pm 123.1441i \tag{62}$$

so that the closed-loop system is asymptotically stable. Note that the open-loop system is unstable, because the first four eigenvalues are zero and the fifth is real and positive.

Next, we consider the observer design. To this end, we first compute the matrix C relating the output vector to the state vector, Eq. (57), and then we use the noise intensity matrices $V = \text{diag}[0.1\ \ 0.001\ \ 0.2\ \ 1\ \ 1\ \ 1\ \ 0\ \ \cdots\ \ 0]$ and $W = \text{diag}[10\ \ 10\ \ 100\ \ 1\ \ 10\ \ \cdots\ \ 10]$ and obtain the observer gain matrix

$$K_o = \left[\begin{array}{ccccccc} 0.0204 & 0 & -0.0002 & 0 & \cdots & 0 & 0 \\ 0 & 0 & 0 & -0.0063 & \cdots & 0 & 0 \\ -0.0015 & 0 & 0.0001 & 0 & \cdots & 0 & 0 \\ 0 & -0.0006 & 0 & 1.3453 & \cdots & 0.0029 & 0.0026 \\ \hline 0 & 0 & 0 & 0 & \cdots & 0 & 0 \\ 0 & 0 & 0 & 0 & \cdots & 0 & 0 \end{array}\right] \tag{63}$$

In general, V and W are computed using actuator and sensor noise signals. In the absence of such signals, V and W must be assumed. The reduced system order rendered this choice much easier. Subsequently, we compute the observer eigenvalues

$$\lambda_{1,2} = -0.1678 \pm 0.1143i, \qquad \lambda_3 = -0.2760$$
$$\lambda_4 = -0.6117, \qquad \lambda_5 = -1.4715, \qquad \lambda_6 = -1.9423$$
$$\lambda_{7,8} = -0.3706 \pm 2.7802i, \ldots,$$
$$\lambda_{27,28} = -9.3140 \pm 123.1433i \tag{64}$$

The eigenvalues are real and negative and complex with a negative real part, which guarantees asymptotic convergence of the estimated state to the actual state.

Finally, we simulate the aircraft response to a gust in the form of an initial impulse distributed over the wing as follows:

$$\boldsymbol{f}_w^R\left(x_w^R, t\right) = \left[0 \quad 0 \quad -0.5\left(3 + x_w^R / L_w\right)\delta(t)\right]^T, \quad 0 < x_w^R < L_w$$
$$\boldsymbol{f}_w^L\left(x_w^L, t\right) = \left[0 \quad 0 \quad -0.5\left(3 - x_w^L / L_w\right)\delta(t)\right]^T, \quad 0 < x_w^L < L_w \tag{65}$$

where the superscripts R and L denote the right half and left half of the wing, respectively, $\delta(t)$ is the Dirac delta function, and L_w is the length of the half wing. Inserting Eqs. (65) into Eqs. (32), we obtain the first-order generalized forces entering into $\boldsymbol{F}_{\text{ext}}$. Then, letting the initial state $\boldsymbol{x}^{(1)}(0)$ be zero, the response to the gust given by Eqs. (65) is obtained by evaluating the convolution integral, Eq. (45). Figures 4 and 5 show the actual and estimated responses for a selected number of rigid-body and elastic variables, where "actual" and "estimated" refer to responses without and with the use of an observer, respectively. As can be seen, convergence of the estimated variables to the actual ones is relatively fast. Moreover, Figs. 6 and 7 show the control inputs.

B. Level Steady Turn Maneuver

In the zero-order problem for the level steady turn maneuver, the aircraft flies at a constant velocity around a circular path of constant radius R in the horizontal XY plane. In this case, it is convenient to refer the rigid-body motions to a set of axes xyz obtained from XYZ through a rotation $\psi^{(0)}$ about Z, where $\dot{\psi}^{(0)} = \Omega = \text{constant}$

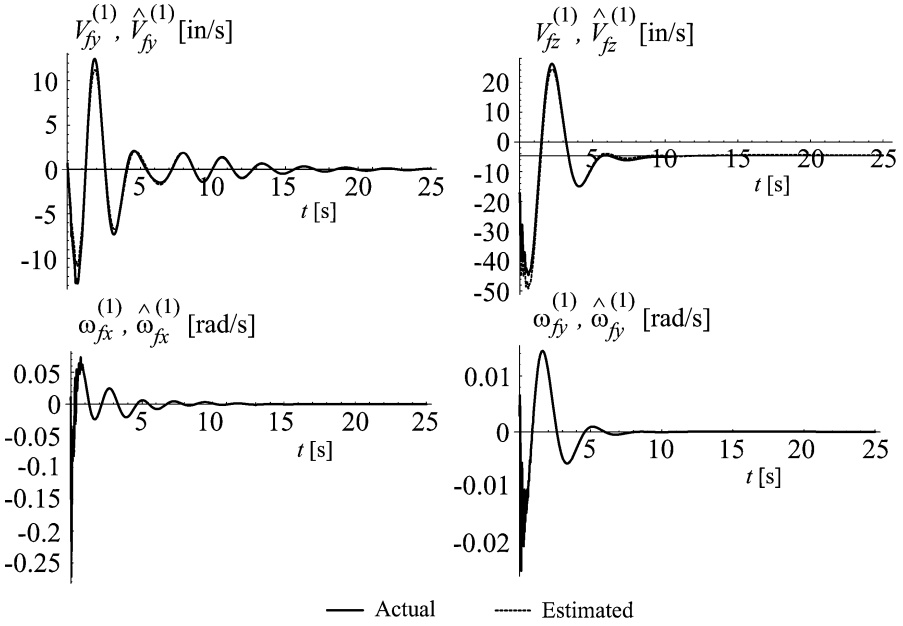

Fig. 4 Sideslip, plunge, roll, and pitch velocities.

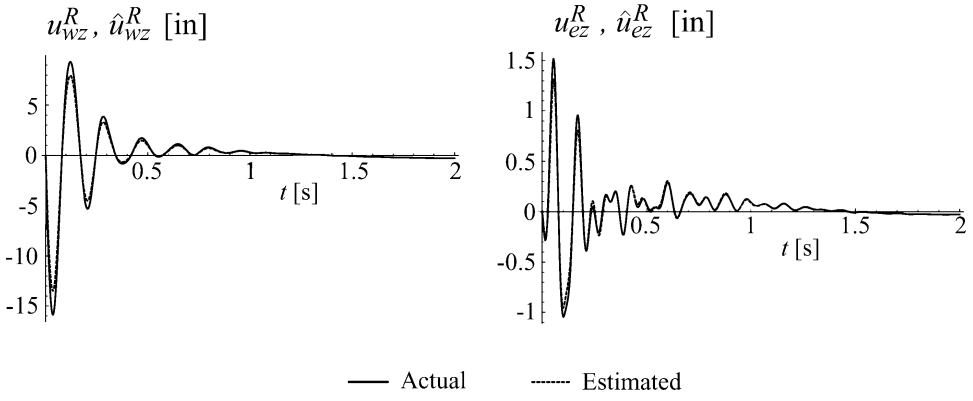

Fig. 5 Wing and elevator tip bending displacements.

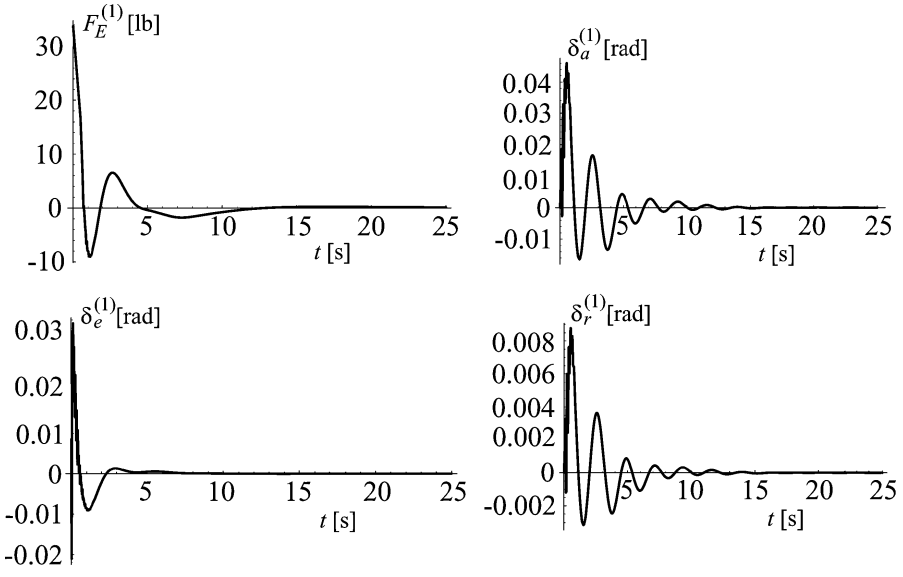

Fig. 6 Engine thrust and aileron, elevator, and rudder angles.

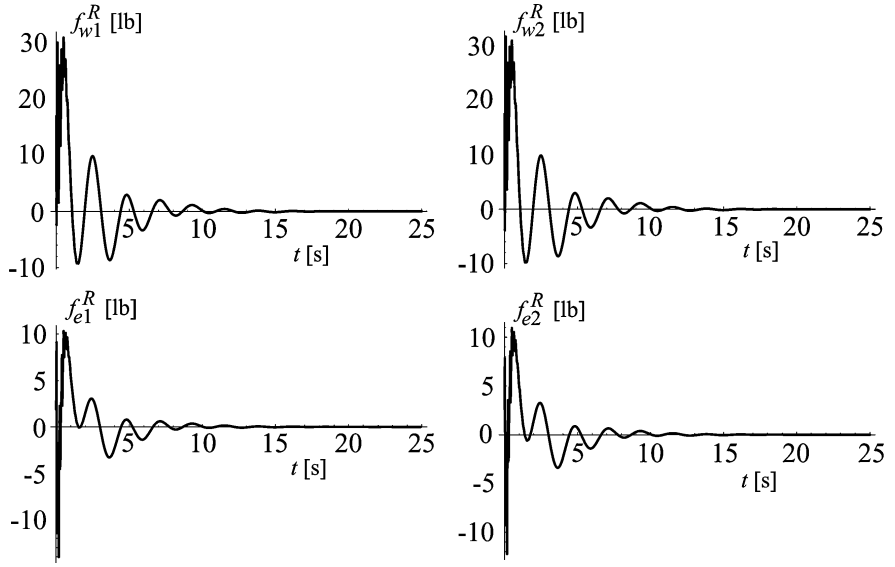

Fig. 7 Wing and empennage control forces.

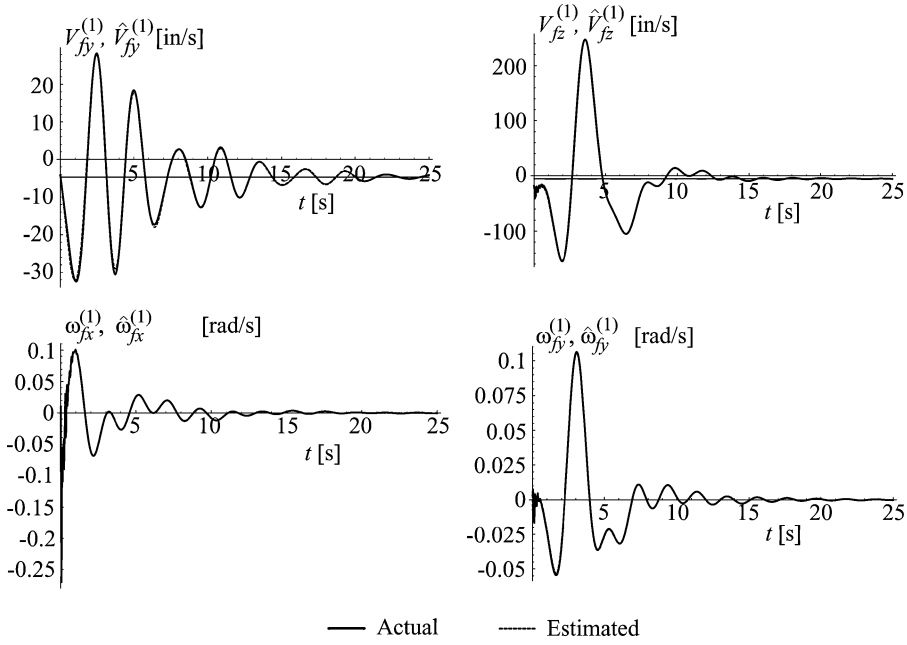

Fig. 8 Sideslip, plunge, roll, and pitch velocities.

is the turn velocity. It follows that the zero-order velocities are

$$\boldsymbol{V}_f^{(0)} = \bar{C}_f^{(0)}[R\Omega \quad 0 \quad 0]^T = \text{const.}$$
$$\boldsymbol{\omega}_f^{(0)} = E_f^{(0)}[0 \quad 0 \quad \Omega]^T = \text{const.} \tag{66}$$

where $\bar{C}_f^{(0)}$ is obtained from $C_f^{(0)}$ by setting $\psi^{(0)} = 0$. From Eqs. (30), the zero-order momenta are

$$\boldsymbol{p}_{Vf}^{(0)} = m\boldsymbol{V}_f^{(0)} + \tilde{S}^{(0)T}\boldsymbol{\omega}_f^{(0)} = \text{const.}$$
$$\boldsymbol{p}_{\omega f}^{(0)} = \tilde{S}^{(0)}\boldsymbol{V}_f^{(0)} + J^{(0)}\boldsymbol{\omega}_f^{(0)} = \text{const.} \tag{67}$$

so that the zero-order equations of motion, second line of Eqs. (27), reduce to

$$-\tilde{\omega}_f^{(0)}\boldsymbol{p}_{Vf}^{(0)} + \boldsymbol{F}^{(0)} = \boldsymbol{0}, \qquad -\tilde{V}_f^{(0)}\boldsymbol{p}_{Vf}^{(0)} - \tilde{\omega}_f^{(0)}\boldsymbol{p}_{\omega f}^{(0)} + \boldsymbol{M}^{(0)} = \boldsymbol{0} \tag{68}$$

We consider the case in which the turn radius is $R = 1.5$ mi $=$ 7920 ft and the tangential velocity is $R\Omega = 416.67$ ft/s, so that the angular velocity of the aircraft during the turn is $\Omega = 0.0526$ rad/s. Inserting Eqs. (66) and (67) in conjunction with these values into Eqs. (68) and solving the resulting nonlinear equations, we obtain the pitch angle, which is equal to the angle of attack, $\theta^{(0)} = 5.65$ deg, the roll angle, which is equal to the bank angle, $\phi^{(0)} = 35.30$ deg, the engine thrust $F_E^{(0)} = 468.7429$ lb, the aileron angle $\delta_a^{(0)} = -0.16$ deg, the elevator angle $\delta_e^{(0)} = -18.53$ deg, and the rudder angle $\delta_r^{(0)} = -19.74$ deg.

As in the case of steady level flight, here too the aircraft experiences small static deformations due to the zero-order forces. The procedure for determining them is described in Ref. 5.

Following the pattern established for steady level flight in conjunction with a reduced-order model with $m = 8$ aircraft shape functions, we can calculate the system matrices A and B. Then, using the weighting matrices $Q = \text{diag}[1 \;\; 1 \;\; \cdots \;\; 1 \;\; 0 \;\; 0 \;\; \cdots \;\; 0]$ and $R = \text{diag}[0.5 \;\; 4 \times 10^7 \;\; 10^7 \;\; 5 \times 10^6 \;\; 50 \;\; \cdots \;\; 50]$ in the performance measure and following the steps outlined earlier, we obtain the gain matrix

$$G = \begin{bmatrix} 1.3996 & -0.1787 & -0.0941 & 62.9719 & \cdots & 0 & -0.0003 \\ 0 & 0.0001 & 0.0001 & 0.4731 & \cdots & 0 & 0 \\ 0 & -0.0002 & 0.0002 & 0.2105 & \cdots & 0 & 0 \\ 0 & 0.0001 & 0 & 0.1472 & \cdots & 0 & 0 \\ 0.0060 & 0.0315 & 0.0223 & 147.4389 & \cdots & -0.0001 & 0.0007 \\ 0.0059 & 0.0293 & 0.0255 & 150.7415 & \cdots & -0.0001 & 0.0007 \\ -0.0050 & -0.0287 & -0.0259 & -150.3271 & \cdots & 0.0001 & -0.0007 \\ \hline 0 & -0.0035 & -0.0016 & -1.7485 & \cdots & 0 & 0 \\ 0.0008 & 0.0010 & 0.0018 & 16.1500 & \cdots & 0 & 0.0001 \end{bmatrix} \tag{69}$$

Then, solving the closed-loop eigenvalue problem (49), we obtain the closed-loop eigenvalues

$$\lambda_{1,2} = -0.2055 \pm 0.1949i, \qquad \lambda_{3,4} = -0.2285 \pm 0.3610i$$

$$\lambda_5 = -0.4546, \qquad \lambda_{6,7} = -0.5963 \pm 0.5315i,$$
$$\ldots, \lambda_{27,28} = -9.3233 \pm 123.1273i \tag{70}$$

so that the closed-loop system is asymptotically stable.

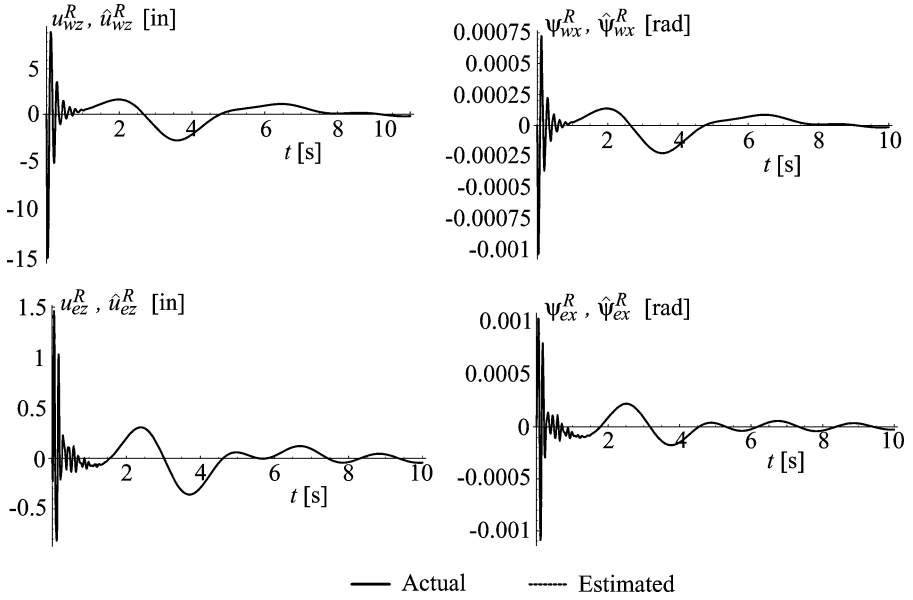

Fig. 9 Wing and elevator tip bending displacements.

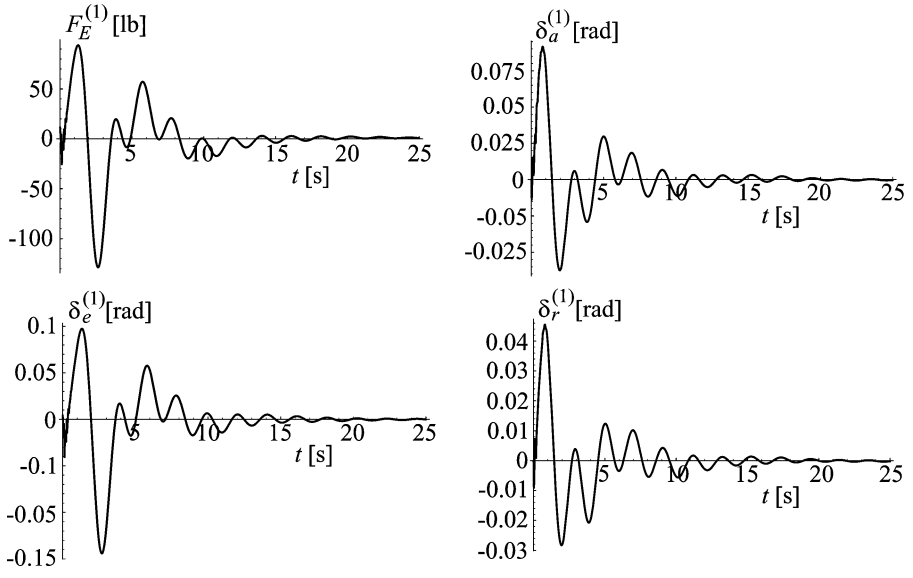

Fig. 10 Engine thrust and aileron, elevator, and rudder angles.

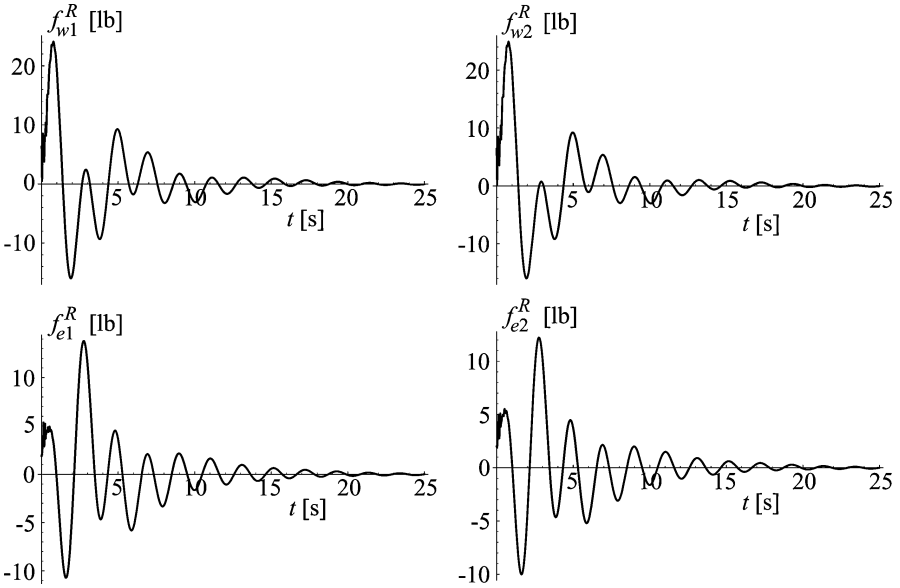

Fig. 11 Wing and empennage control forces.

Turning our attention to the observer design, we first compute the matrix C according to Eq. (57). Then, using the noise intensity matrices $V = \text{diag}[10^{-5}\ \ 10^{-6}\ \ 10^{-6}\ \ 1\ \ 1\ \ 1\ \ 0\ \ 0\ \ \cdots\ \ 0]$ and $W = \text{diag}[10\ \ 10\ \ 5\ \ 5\ \ 10\ \ \cdots\ \ 10]$, we obtain the observer gain matrix

$$K_o = \left[\begin{array}{cccccccccc} 0 & 0 & 0 & 0.0001 & -0.0010 & 0 & \cdots & 0 & 0 \\ 0 & 0 & 0 & -0.0001 & 0 & 0.0003 & \cdots & 0 & 0 \\ 0 & 0 & 0 & -0.0001 & -0.0001 & 0 & \cdots & 0 & 0 \\ 0.0001 & 0 & -0.0001 & 0.4970 & -0.0658 & -0.0997 & \cdots & 0.0067 & 0.0060 \\ -0.0010 & 0 & -0.0001 & -0.1317 & 2.0082 & -0.0061 & \cdots & 0.0003 & 0.0007 \\ 0 & 0.0003 & 0 & -0.1994 & -0.0061 & 1.7912 & \cdots & 0.0115 & 0.0105 \\ \hline 0 & 0 & 0 & 0 & 0 & 0 & \cdots & 0 & 0 \\ 0 & 0 & 0 & 0 & 0 & 0 & \cdots & 0 & 0 \end{array}\right] \tag{71}$$

and subsequently the observer eigenvalues

$$\lambda_1 = -0.0044, \qquad \lambda_{2,3} = -0.2002 \pm 0.1823i$$

$$\lambda_{4,5} = -0.4829 \pm 0.6877i, \qquad \lambda_{6,7} = -0.9946 \pm 0.9116i,$$

$$\ldots, \lambda_{27,28} = -9.3191 \pm 123.1265i \tag{72}$$

indicating asymptotic stability of the observer. Next, we simulate the aircraft response to the same gust as given by Eqs. (65). Figure 8 shows actual and estimated rigid body velocities and Fig. 9 displays wing and elevator tip bending and torsional displacements; the torsional displacements are quite small. As can be seen, convergence of the observed state to the actual state is quite fast. In addition, Fig. 10 shows the first-order engine thrust and the aileron, elevator, and rudder angles and Fig. 11 shows the feedback control forces on the right half-wing and on the right half-elevator.

Conclusions

Quite recently, the authors developed a unified formulation for the dynamics and control of maneuvering flexible aircraft.[5] The formulation represents a seamless integration of pertinent material from analytical dynamics, structural dynamics, aerodynamics, and controls. It includes both the aircraft rigid-body motions and elastic deformations, as well as the aerodynamic, gravity, propulsion, and control forces, all in a rigorous manner. The formulation permits time simulations of the response of maneuvering flexible aircraft to initial conditions and external excitations.

There is a basic conflict in requirements between structural and aerodynamic modeling on the one hand and feedback control on the other hand. Indeed, structural and aerodynamic modeling tend to require a large number of variables, whereas control design experiences serious difficulties with high-dimensional systems. This paper contains improvements over an earlier formulation. In particular, by using a Galerkin spatial discretization in conjunction with whole-aircraft shape functions, the number of states has been reduced from 76 to 28. This is a significant reduction in view of the fact that it all came from the elastic states, because the number of rigid-body states remained the same at 12. In turn, the reduced-order system permitted better controller and observer designs, resulting in better aircraft performance, as can be seen from the time simulations. Moreover, there is a significant reduction in the computational effort.

It is perhaps appropriate to point out here that the theory developed by the authors is concerned with a dynamic synthesis for flexible aircraft, and in particular with how the individual disciplines are made to work together as a single system, the ultimate objective being on-line or real-time simulations of the aircraft response. The disciplines involved are analytical dynamics, structural dynamics, aerodynamics, and controls. Note that, because the formulation is modular in nature, the structural modeling, aerodynamic theory, and control method can be replaced by other ones to suit a given type of aircraft, provided the replacements lend themselves to ready integration into the unified formulation. One discipline particularly difficult to integrate into the unified formulation is aerodynamics, which has

developed a life of its own and is notorious for time-consuming computations. In fact, for seamless integration into a unified formulation and for the ability to compute aerodynamic forces in such a way as to permit sufficiently fast time simulations, it appears that a new aerodynamic methodology is necessary. Until such new theory becomes available, this paper uses strip theory to demonstrate the integration process.

The aircraft model used here, Fig. 1, is that of an executive jet. Yet the theory developed by the authors is able to accommodate aircraft intended for considerably more critical missions than a transport aircraft performs. Indeed, the developments are ideally suited to autonomously controlled unmanned aerial vehicles (UAVs), for which all control decisions must be made by autopilots. Real-time simulations and feedback control by means of observers are needed for autopilot control of the type envisioned here. In this regard it should be pointed out that all the time simulations in this paper were carried out by a 1-GHz personal computer.

Acknowledgments

This research was carried out under NASA Cooperative Agreement NCC-1-346, monitored by M. R. Waszak, Dynamics and Control Branch, Langley Research Center.

References

[1]Meirovitch, L., "Hybrid State Equations of Motion for Flexible Bodies in Terms of Quasi-Coordinates," *Journal of Guidance, Control, and Dynamics*, Vol. 14, No. 5, 1991, pp. 1008–1013.

[2]Meirovitch, L., "A Unified Theory for the Flight Dynamics and Aeroelasticity of Whole Aircraft," *Proceedings of the Eleventh VPI&SU Symposium on Structural Dynamics and Control*, Virginia Polytechnic Inst. and State Univ., Blacksburg, VA, 1997, pp. 461–468.

[3]Etkin, B., *Dynamics of Flight*, 2nd ed., J. Wiley, New York, 1982, Chap. 4.

[4]Dowell, E. H. (ed.), *A Modern Course in Aeroelasticity*, 3rd ed., Kluwer Academic, Dodrecht, The Netherlands, 1995.

[5]Meirovitch, L., and Tuzcu, I., "Unified Theory for the Dynamics and Control of Maneuvering Flexible Aircraft," *AIAA Journal*, Vol. 42, No. 4, 2004, pp. 714–727; also NASA CR-2003-211748, June 2003.

[6]Fornasier, L., Rieger, H., Tremel, U., and van der Weide, E., "Time-Dependent Aeroelastic Simulation of Rapid Manoeuvring Aircraft," AIAA-2002-0949, Jan. 2002.

[7]Meirovitch, L., *Principles and Techniques of Vibrations*, Prentice–Hall, Upper Saddle River, NJ, 1997, Chap. 8.

[8]Meirovitch, L., *Methods of Analytical Dynamics*, Dover, New York, 2003, Chap. 3.

[9]Meirovitch, L., *Dynamics and Control of Structures*, Wiley-Interscience, New York, 1990, Chap. 6.